VOLUME 4 ISSUE 2 JUNE 2019

IJEG

International Journal of Engineering and Geosciences

e-ISSN 2548-0960

The International Journal of Engineering and Geosciences (IJEG)

The International Journal of Engineering and Geosciences (IJEG) is a tri-annually published journal. The journal includes a wide scope of information on scientific and technical advances in the geomatics sciences. The International Journal of Engineering and Geosciences aims to publish pure and applied research in geomatics engineering and technologies. IJEG is a double peer-reviewed (blind) OPEN ACCESS JOURNAL that publishes professional level research articles and subject reviews exclusively in English. It allows authors to submit articles online and track his or her progress via its web interface. All manuscripts will undergo a refereeing process; acceptance for publication is based on at least two positive reviews. The journal publishes research and review papers, professional communication, and technical notes. IJEG does not charge for any article submissions or for processing.

CORRESPONDENCE ADDRESS
Journal Contact: engineeringandgeoscience@gmail.com

CONTENTS

Volume 4 - Issue 2

ARTICLES

International Journal of Engineering and Geosciences (IJEG),
Vol; 4, Issue; 2, pp. 052-057, June, 2019, ISSN 2548-0960, Turkey,
DOI: 10.26833/ijeg.446912

ANALYZING THE URBANIZATION IN THE PROTECTION AREA OF THE BOSPHORUS

Cigdem Goksel[1]*, Ahmet Ozgur Dogru[1]

[1]Istanbul Technical University, Department of Geomatic Engineering, Istanbul, Turkey

(goksel@itu.edu.tr ozgur.dogru@itu.edu.tr); **ORCID -0000-0001-8480-1435 ; ORCID 0000-0001-7415-1862**

*Corresponding Author, Received: 23/07/2018, Accepted: 13/08/2018

ABSTRACT: Istanbul, being one of the oldest and crowded cities in the world bridging the Asia and Europe continents, is ranked as the 15th populated mega city among the 75 largest metropolitans in the world as a result of the rapid population growth since the year of 1950. The stated growth caused a significant need for housing, therefore new settlements have been built in and around the city threating water resources, protected areas, and sensitive lands such as agricultural areas, forests, wetlands in the city. As a result of these adverse developments, the Bosphorus zone, which has a historical and geographical importance for Istanbul, was declared as a protected zone for stopping the threat of unplanned urbanization along the Bosphorus. The Bosphorus area were divided in to two protection zones as Back View and Front View Zones by the laws in terms of the stated protection plan. The main goal of this study is to examine the changes in settlement areas in the protected zones of Bosphorus specifically in Sariyer District. In this context, Landsat imageries dated 2005 and 2017 were used to determine the urban sprawl during 12 years in the protection zone of Bosphorus. The results of the study introduced 10% decrease in the forest and green lands from 2005 to 2017 while 8% and 11% increase in settlements and the other land use classes respectively. In order to perform more detailed analyses of this change, a detailed study was performed for Front and Back View Zones of Bosphorus in Sariyer district using 2005 and 2017 dated IKONOS satellite images. The map of Sariyer district produced in 1960 was considered as the reference data source as well as image for detecting the changes in the study area during 57 years in two periods. The results of the study outlined that the settlements in the study area increased 173% and 142% for two periods from 1960 to 2005 and from 2005 to 2017 respectively. The increase in settlement areas caused a decrease in forests and green lands in the study area. In particular, the study introduced the illegal settlement area increase in the protection zones of the Bosphorus based on the Bosphorus Law No. 2960 in Sariyer District.

Keywords: *Remote Sensing, Change Detection, Urbanization, Urban Sprawl*

1. INTRODUCTION

Istanbul Strait, in other words the Bosphorus, is a unique territory with its topographic features, historical characteristics, green spaces, living coastline, architectural features and urban texture and it should be extensively protected by regulations and law. The Bosphorus has maintained its importance as a settlement area throughout history and it has also provided a living space for inhabitants with surrounding plantations. Therefore, organizations responsible for the urban planning have considered the protection of the natural and cultural heritage at Bosphorus area while providing development plans of the area since 1970s. However, these attempts have not fully succeeded as a result of grooving population mostly caused by internal migration, inconsistencies in plans and protection orders or interventions of the political actors. Consequently, the Bosphorus have been under the threat of legal or illegal urbanization and industrialization for many years.

As a precaution, the Bosphorus Law No. 2960 came in to force on 18th November 1983 for the governance of the rapid urbanization at the Bosphorus area. According to the law, the Bosphorus area were divided in to four parts as water side, Front View, Back View and Effect Zones as presented in Figure 1. The Bosphorus area was considered as recreation, tourism and settlement area with this law and decided to be legally protected with its existing natural and historical characteristics (Gülersoy and Selçuk, 1993; Kap, 2008). However, an urban design guide was prepared for an area including private owned green areas with construction permissions and this guide was confirmed by the cultural and natural heritage preservation board (Gülersoy, 1995; Gökçek, 1992; IBB, 2007). These prevention attempts were interrupted by Development Plan Law Num. 3194 which was enacted in 1985 after the inurement of the Bosphorus Law since it legislated all previous illegal acts and opened some areas in the protection zone for settlement. Therefore, the period after the year 1985 was considered as rapid urbanization period of the Bosphorus area (Örmeci et al., 1996).

The first goal of this study is to determine the land use / land cover (LU/LC) changes in especially settlement and green areas in the protection area of the Bosphorus for last 12 years from 2005 to 2017 by processing and analysing Landsat TM and ETM images. Additionally, this study aims to detect the changes in Kirecburnu and Buyukdere neighbourhoods located at a part of Front View and Back View Zones of the Bosphorus in Sariyer where urbanization highly effected for years. For this purpose, 2005 and 2017 dated IKONOS imagery data with 1 m spatial resolution were used in order to obtain more accurate results. The changes in urban and green areas were analysed based on 1:5000 scaled topographic maps of Istanbul dated 1960 in the second part of the study.

2. STUDY AREA

The Bosphorus preservation areas have a significant importance a natural and cultural heritage of Istanbul. This region included Sariyer and Beşiktaş districts in European side and Beykoz and Uskudar districts in Asian side of Istanbul. The area has been threatened by unplanned and illegal urbanization since 1950s. According to the Bosphorus Law No. 2960, the Bosphorus was divided in to four main regions as coastal line, Front View Zone, Back View Zone and Effect Zone. Front View Zone of the Bosphorus included most important preservation areas and it covered an area of 4300 ha, while Back View Zone covered an area of 1000 ha located between Front View Zone and Effect Zone which formed border zone of 5300 ha between the urban and rural areas of Istanbul when the Bosphorus Law enacted. Figure 1 presents the extended study area borders as the Front View and Back View Zones at the Bosphorus. The study mainly focused on the Front View and Back View Zones at Sariyer District.

3. METHODOLOGY AND DATA PROCESSING

Satellite remote sensing is a potentially powerful means of monitoring land-use change at high temporal resolution and economic than those associated with the use of traditional methods (El-Raey et al., 1995).

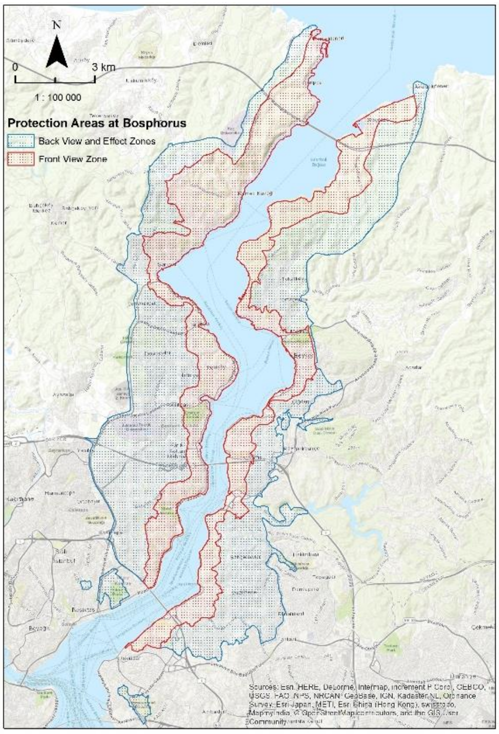

Figure 1. Front View, Back View and Effect Zones at the Bosphorus (adapted from Vural, E. 2008)

Digital change detection is the process of determining and/or describing changes in LU/LC properties based on co-registered multi-temporal remote sensing data. The basic premise in using remote sensing data for change detection is that the process can identify change between two or more different dates. Numerous researchers have addressed the problem of monitoring LU/LC change (Yuan et al., 2005; Bektas and Goksel, 2005, Dogru et al., 2009; Belal, and Moghanm, 2011).

In this study Landsat TM (2005), Landsat 8 OLI (2017) and IKONOS images were used as the geometric data as well as 1:5000 scaled topographic map sheet covering some part of the Sariyer District which was produced in 1960 and used as the basic reference data for introducing LU/LC change in 57 years. ERDAS Imagine 9.2 software were used for processing remote sensing imageries. Digitization and the georeferencing of the topographic map and visualization of the results as final map were succeeded using ArcMap 10.6.

Satellite data used in the study were processed at four main stages as: geometric correction of remotely sensed images and maps as data pre-processing, classification of the satellite images together with its accuracy assessment and digitization.

3.1 Geometric Correction of Satellite Images

As the first step of the geometric correction high resolution IKONOS satellite images used this study were geometrically referenced to a common coordinate system defined in a projection. For this purpose, 1:5000 scaled orthophoto maps were used as reference data and ground control points were rigorously selected as homogenously distributed on the image. As a result of this process 2005 and 2017 dated IKONOS images were georeferenced to Universal Transverse Mercator (UTM) projection based on the World Geodetic System 1984 (WGS 84) datum. International ellipsoid 1909 was selected as reference ellipsoid of the data. Nearest Neighbour Interpolation were applied at the resampling stage for ensuring a minimum change in spectral values of the images. This process was completed with a root mean square error (RMSE) of ±0.5 pixel for both images. Additionally, 2005 and 2017 dated Landsat images used in the study were geometrically corrected using 15 ground control points for each based on 2005 dated IKONOS image with 0.5 pixel RMSE.

3.2 Geometric Correction of Maps

The study aims at the integration of the information derived from existing analogue maps with remote sensing data defined at a common coordinate system for providing more detailed interpretation of the results. In this context, two 1:5000 scaled analogue maps dated 1960 was first scanned and then georeferenced using Geographic Information System (GIS) technology within this study. For this purpose, maps in raster format were transformed in to UTM projection system using polynomial transformation methodology (Lillesand and Kiefer, 2001). A number of graphical elements of spatial objects were identified and selected as control points and check points on each data. Ground control point (GCP) selection process included two important problems (Goksel et al., 2016). Firstly, it was difficult to find out the GCP because of the change at the field occurred in 45 years' period from 1960 to 2005. Secondly, the GCP was not selected on the homogeneous distribution in the area. As a result, geometrical correction of the raster maps was performed using 6 GCP with 0.4 pixel RMSE.

3.3 Classification and Accuracy Assessment

Image classification techniques are widely used in determining land use and land cover changes (Goksel, et al., 2018; Karakuş, et al., 2017). In this study, Landsat images with 30m spatial resolution used for determining LU/LC characteristics of Bosphorus protection zone in 2005 and 2017. For this purpose; Maximum likelihood supervised classification methodology was applied in order to map main LU/LC characteristics of the study area as (i) green lands and forests (ii) settlement- urban built up and roads and (iii) others. The change in between the years was also calculated after completing classification process. The error matrix and Kappa methods were used to assess the thematic mapping accuracy. Accuracy assessment of the LU/LC classification succeeded with 87% and 81% overall accuracies for 2005 and 2017 dated Landsat data respectively. The Kappa coefficients for 2005 and 2017 maps were also obtained as 0.803 and 0.745 respectively.

3.4 Digitization

In order to determine the areal change in settlement area based on building area in Sariyer district, most of the buildings located at Sariyer Center, Tarabya and Camlıtepe neighbourhoods and all of the buildings located at Kazim Karabekir, PTT Evleri, Maden, Kocatas, Buyukdere, Cayirbasi, Cumhuriyet, Kirecburnu neighbourhoods were manually digitized from both raster maps and high resolution IKONOS images. After completing the digitization of the settlement data changes in settlement are in Sariyer District were determined (Goksel et al. 2016).

4. RESULTS

Results of the study are obtained in two different scopes: firstly, general overview of the LU/LC changes in Bosphorus Protection Zone and secondly detailed examination of the Sariyer District. LU/LC classification results of the Bosphorus protection Zone is visualized as LU/LC maps of the study area in Figure 2. The numeric results were also presented in Table 1 by grouping four LU/LC classes in to three classes as Forest and Green Areas, Settlements-Urban Builtup & Roads and Others. As presented in the table, while Forest and Green Areas in Bosphorus Protection Zone decreased 526.5 ha with a -10.1% rate in 12 years Settlements and Roads increased 449.5 ha. This result confirms the illegal urbanization at the Bosphorus protected by laws.

International Journal of Engineering and Geosciences (IJEG),
Vol; 4, Issue; 2, pp. 052-057, June, 2019,

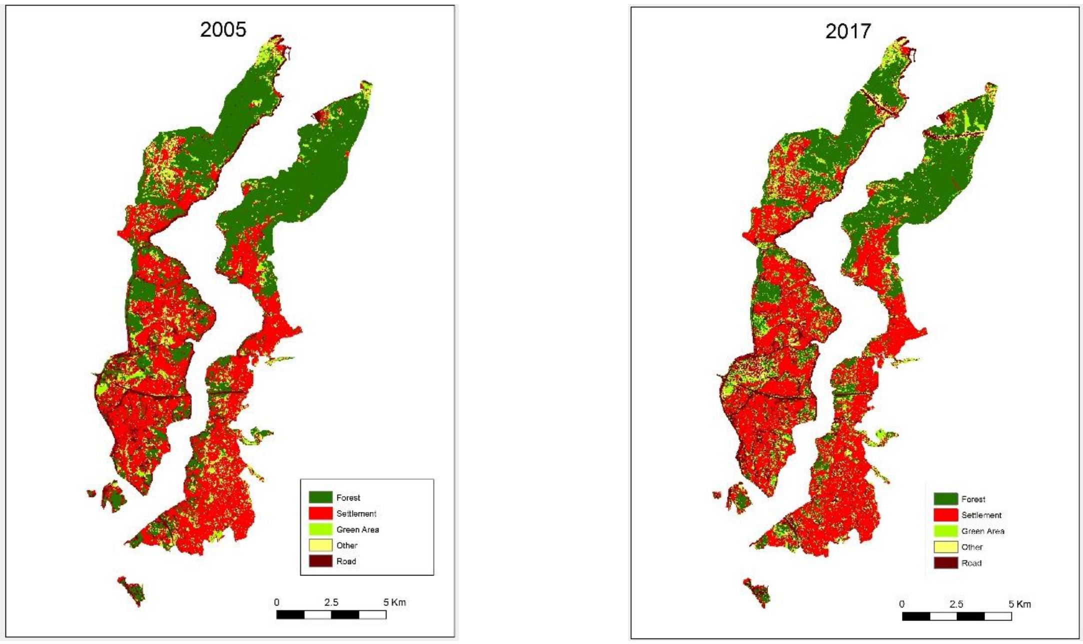

Figure 2. 2005 and 2017 dated LU/LC maps of the Bosphorus Protection Zones

Table 1. Areas of LU/LC classes and change in 12 years in Bosphorus Protection Zone

LU/LC Class	2005		2017		Change	
	ha	% in study area	ha	% in study area	ha	%
Forest and Green Areas	5229.1	46.1	4702.6	41.5	-526.5	-10.1
Settlements and Roads	5414.4	47.7	5863.4	51.7	449.0	8.3
Others	698.0	6.2	775.5	6.8	77.5	11.1
Total	11341.5		11341.5			

Results of the examination of the urbanization processes in Sariyer District were presented in Figure 3 and Table 2. Map in the Figure 3 presents the digitization results of building areas in 1960, 2005 and 2017 in three different colures. A numerical comparison of the building areas in 1960, 2005 and 2017 were also presented in Table 2. As presented in the table building areas in located at the Back View and Front View Zone in the study area increased with rates of 173% and 142% in two study periods. Total increase rate in settlement areas from 1960 to 2017 was determined as 420% from 15 ha to 78 ha.

Table 2. Comparison of settlement areas

<table>
<tr><th>Years</th><th>Settlement Area by Year (ha)</th><th>Total Settlement Area (ha)</th><th>Increase Rate (%)</th></tr>
<tr><td>1960</td><td>15</td><td>15</td><td rowspan="2">173</td></tr>
<tr><td>2005</td><td>26</td><td>41</td></tr>
<tr><td>2017</td><td>37</td><td>78</td><td>142</td></tr>
</table>

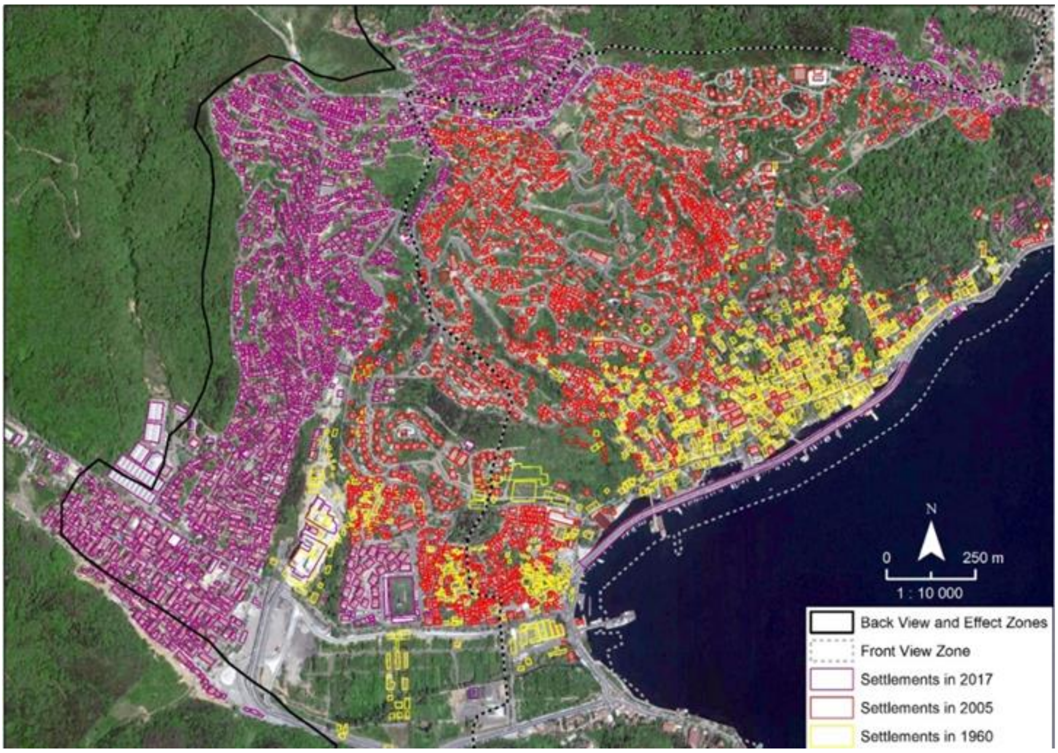

Figure 3. Building areas in three different years

5. CONCLUSION

This study confirms the usability of the data sets from different sources and formats in studies performed for detecting the LC/LU change. A wide variety of maps as urban development plans or topographic maps in analogue or digital formats and produced using traditional or current mapping methodologies, as remote sensing or aerial photography, can be efficiently used in change detection. The main requirement for the success of such data uses is to define and structure the all geometric data at a common geographic reference system. In this study, many challenges of georeferencing, map matching and digitizing processes mainly originated by the deformations on paper maps were succeeded.

As a result of the change detection process, it is concluded that the green areas and forests in the preservation area of the Bosphorus were significantly damaged in 12 years' time from 2005 to 2017. These results indicated the increase in settlement areas (8.3%) replaced with forests and green areas. Building area increased with 223% in 45 years' time from 1960 to 2005 also confirms this result. The census statistics of TUIK presents more than 450% increase in Sariyer's population at the same period (URL 1) and this result indicated the increase in the number of multi-storey building in the study area. Consequently, determined change is the exact indicator of the difficulties in application of the laws and legislation as the Bosphorus Law, Bosphorus development plans and etc. on preservation of the economically and culturally most valuable area in Istanbul.

REFERENCES

Bektas, F., and Goksel, C. (2005). Remote Sensing And GIS Integration For Land Cover Analysis, A Case Study: Bozcaada Island. *Water Science and Technology*, 51(11), 239–244.

Belal, A.A., Moghanm, F.S. (2011). Detecting Urban Growth Using Remote Sensing And GIS Techniques In Al Gharbiya Governotare, Egypt. *The Egyptian Journal of Remote Sensing and Space Sciences*,14, 73–79.

Dogru, A.O., Balcik, F., Sanli, F., Goksel, C., Ulugtekin, N. (2009). A Change Detection Analysis in the Izmir Bird Paradise: Integration of Remote Sensing and Geographic Information System. *Fresenius Environmental Bulletin (FEB),* Vol 18, No 1, pp. 51 – 56,

EL-RAEY, M., Nasr, S. M., El-Hattab, M. M., & Frihy, O. E. (1995). Change detection of Rosetta promontory over the last forty years. Remote Sensing, 16(5), 825-834.

Gökçek, G. (1992). Boğaziçi Plan Kararlarının İrdelenmesi ve Bu Kararların Yapı, Doku ve Silüet ile İlişkilenmesi Sariyer Örneği, Master Thesis, MSÜ Institute of Science and Technology.

Goksel, C., Dogru A. O. and Vural, E. (2016) "Analyzing The Urbanization In The Forescene And Backscene Zone Of The Bosphorus In Sariyer District". *Proceedings, Selçuk International Scientific Conference On Applied Sciences*, 27-30 September 2016, Antalya-Turkey

Gülersoy, N,Z. (1995). Boğaziçi'nde Arazi Kullanımı ve Ulasım, *Istanbul Dergisi,* No: 14, Tarih Vakfı, pp.59-63.

Gülersoy,N.Z., Selçuk, Z. (1993) "Istanbul Boğaziçi Koruma Alanında 1970-1990 Yılları Arasındaki Gelişmelerin Değerlendirilmesi". *Türkiye'de 17. Dünya Şehircilik Günü Kolokyumu Bildiriler Kitabı*. pp. 345-362.

IBB, 2007, Istanbul Metropolitan Municipality Strategic Plan for 2002-2011 period, available at: http://www.sp.gov.tr/upload/xSPStratejikPlan/files/2dWVM+IstanbulBuyuksehirSP20072011.pdf, last accessed on 14.08.2016.

Kap, S.D. (2008). "The Effect of the Legal Arrangements on the Istanbul Bosphorus Landscape Areas and European Landscape Convention as an Opportunity for Restructuring". Proceeding of *1st WSEAS International Conference on Landscape Architecture (LA '08),* Algarve, Portugal, June 11-13, 2008. Pp.183-188

Göksel, Ç., David, R.M. and Dogru, A. O.(2018) "Environmental Monitoring of Spatio-Temporal Changes in Northern Istanbul using Remote Sensing and GIS". International Journal of Environment and Geoinformatics 5(1): 94-103 (2018)

Karakus, P., Karabork, H., & Kaya, S. (2017). A Comparison Of The Classification Accuracies In Determining The Land Cover Of Kadirli Region Of Turkey By Using The Pixel Based And Object Based Classification Algorithms. International Journal of Engineering and Geosciences (IJEG), 2, 52-60.

Lillesand, T.M. and Kiefer, R.W. (2001). Remote Sensing and Image Interpretation, John-Wiley and Sons., New York.

Örmeci, C. Türkoğlu, H. and Göksel, Ç., (1996). "Uzaktan Algılama Yöntemi Kullanılarak İstanbul Boğaziçi'nde Arazi Kullanımındaki Değişimin Analizi". Proceeding of *Istanbul 2020 Syposium*-İTÜ, April 1996, pp:265-273.

URL 1: https://biruni.tuik.gov.tr, Official website of the Turkish Statistical Institute Data/Information Portal, last accessed on 14.08.2016.

Vural, E. (2008). Boğaziçi SİT Alanındaki Arazi Kullanımının Zamansal Değerlendirmesi, *Master Thesis, İTÜ Graduate School of Science Technology and Engineering*.

Yuan, F., Sawaya, K.E., Loeffelholz, B.C., Bauer, M.E., (2005). Land cover classification and change analysis of the twin cities (Minnesota) metropolitan area by multitemporal Landsat remote sensing. *Remote Sensing of Environment.* 98, 317–328.

International Journal of Engineering and Geosciences (IJEG),
Vol; 4, Issue; 2, pp. 058-062, June, 2019, ISSN 2548-0960, Turkey,
DOI: 10.26833/ijeg.446962

INVESTIGATION ON THE EFFECTS OF NUMBER OF COMMON POINTS IN 2D TRANSFORMATION PROBLEM

Taylan Ocalan [1]*

[1]Yildiz Technical University, Civil Engineering Faculty, Department of Geomatic Engineering, İstanbul, Turkey
(tocalan@yildiz.edu.tr); **ORCID 0000-0003-0861-013X**

*Corresponding Author, Received: 23/07/2018, Accepted: 13/08/2018

ABSTRACT: Coordinate transformation from one datum to another is the basic problem in geodesy. Generally, the problem may be expressed by converting coordinates in a cartesian coordinate system with defined origin provided by the intersection of two or three axes into another system using mathematical equations. To compute the transformation parameters, a sufficient number of coordinates of the common points should be known in two systems. The problem involves either 2D or 3D coordinate systems. Traditionally the commonly used model for the estimation of the transformation parameters is the Least Squares (LS) method refers as to Helmert Transformation. This study aims to compare the performance of the spatial distribution and quantity of the common points in LS method for coordinate transformation problems. For this purpose, a geodetic network with 25 points, whose coordinates are commonly known in two datum are used to compute the performance of the transformation problem under the different scenarios. To compare the cases, the sum of the absolute coordinate differences is provided by subtracting the original coordinates of test points from computed coordinates by using estimated transformation parameters. The results show that increasing control points one by one to estimate the transformation parameters improve the results of the transformation parameters and reliable transformation parameters have been estimated when a homogeneously distributed 8 points are taken as common points for about a region as 1500 km^2.

Keywords: *Least Square (LS) Method, Coordinate Transformation, Transformation Parameter, Accuracy*

1. INTRODUCTION

Coordinate transformation is one of the most common issues in geodesy phenomena. It is used to transform coordinates from one datum to other by using parameters as translation terms, scale and rotation angle. The increase of application areas in engineering surveys and integration of layouts with different datum has been increased the necessity of accurate datum transformation. The problem in datum transformation is to compute the transformation parameters using common points with known coordinates into two different datum.

Researchers use a number of strategies in order to estimate transformation parameters. For 2D networks, Helmert Transformation is the most commonly used method. Helmert Transformation employs a linear transformation between two systems (Chen and Hill, 2005). Its parameters are two translation terms along the two axes, scale and rotation angle between the axes of two coordinate systems (Akyilmaz, 2007). In Helmert Transformation, at least two common points that their coordinates are well known both datum are required. The numbers of common points given above are the minimum numbers required for the solution and Helmert Transformation uses Least-Squares (LS) method using these common points' coordinates. Moreover, distribution of common points in both datum provides different datum parameters (Kutoglu and Ayan, 2006), which is significant in estimating transformation parameters (Tan et al., 2013) by LS method (Kutoglu and Vaníček, 2006). Here, the number of the common points to be used in transformation problem is also important. Even though the minimum three common points in both datum should be known for adjustment, in this case, it is seen that the reliability of the results obtained from estimation is low. If the number of the common points are increased for estimation of the transformation parameters, the differences between original and converted coordinates decrease. For this purpose, in this paper, first, the mathematical expressions of 2D coordinate transformations using LS method is introduced. Then, the latter section presents the case study depending on a real network and the results of them. The last section concludes with the analyses of the comparative performances of the LS method. In this study, when the number of the common points reaches 8, which the total number of common points is 11 with a homogeneous geometrical distribution, improved results computed by the differences of the test points have been obtained.

2. *THE MATHEMATICAL MODEL OF 2-D TRANSFORMATION PROBLEM (HELMERT TRANSFORMATION)*

2D Coordinate transformation, so-called Helmert Transformation today, has been formulated by F.R. Helmert, and considers only one system contains error in the stochastic model. The transformation parameters are estimated by the LS method. 2D Helmert transformation problem includes four transformation parameters; two translation terms, one rotation component and one scale factor. To estimate the parameters, common points in two different systems are used. The equations of Helmert Transformation problem are mentioned in Eq. (1) and (2).

$$\boldsymbol{x = t_\chi + k.cos\varepsilon.\chi - k.sin\varepsilon.\gamma} \quad (1)$$
$$\boldsymbol{y = t_\gamma + k.sin\varepsilon.\chi + k.cos\varepsilon.\gamma} \quad (2)$$

Where t_χ and t_γ are translation terms, k is scale factor, ε is rotation component. The sub-matrices of design matrix **A** are written as follow,

$$\boldsymbol{A_i} = \begin{bmatrix} \mathbf{1} & \mathbf{0} & \chi & -\gamma \\ \mathbf{0} & \mathbf{1} & \gamma & \chi \end{bmatrix} \text{ i=1,…..,n} \quad (3)$$

Here, n is the number of common points in both systems. $\boldsymbol{l_i} = [\boldsymbol{x_i} \quad \boldsymbol{y_i}]^{\boldsymbol{T}}, \boldsymbol{i} = \mathbf{1}, \dots, \boldsymbol{n}$ is the observation vector of the transformation problem. To estimate the transformation parameters $\boldsymbol{\hat{\beta}} = [\boldsymbol{t_\chi} \quad \boldsymbol{t_\gamma} \quad \boldsymbol{k.cos\varepsilon} \quad \boldsymbol{k.sin\varepsilon}\ ]^{\boldsymbol{T}}$ the linear observation equation can be formed as follows (Koch, 1999):

$$\boldsymbol{v_{LS} = A\hat{\beta} - l} \quad (4)$$

$$\begin{bmatrix} \boldsymbol{v_\chi} \\ \boldsymbol{v_\gamma} \end{bmatrix} = \begin{bmatrix} \mathbf{1} & \mathbf{0} & \chi & -\gamma \\ \mathbf{0} & \mathbf{1} & \gamma & \chi \end{bmatrix} \begin{bmatrix} \boldsymbol{t_\chi} \\ \boldsymbol{t_\gamma} \\ \boldsymbol{k.cos\varepsilon} \\ \boldsymbol{k.sin\varepsilon} \end{bmatrix} - \begin{bmatrix} \boldsymbol{x} \\ \boldsymbol{y} \end{bmatrix} \quad (5)$$

Once transformation parameters between two systems are estimated by common points, χ and γ coordinates are converted to second system namely x and y coordinates (as seen Fig.1).

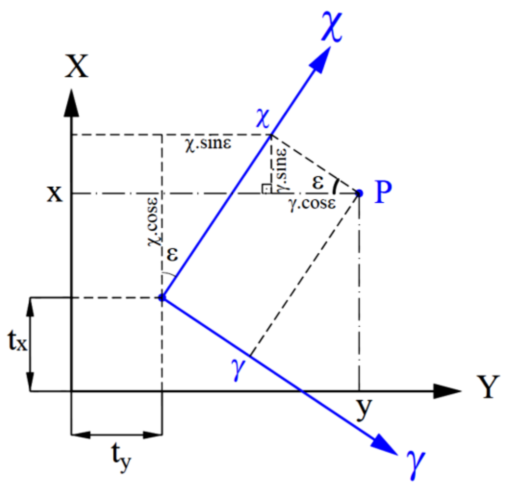

Figure 1. 2D Coordinate Transformation

3. CASE STUDY

For the comparative analysis of computing transformation parameters, a 25-points network established in the Asian side of the İstanbul, Turkey with the known coordinates in both ITRF96 and ED50 has been used. The location of the study area is represented in Figure 2. The total area is about 1450 km^2.

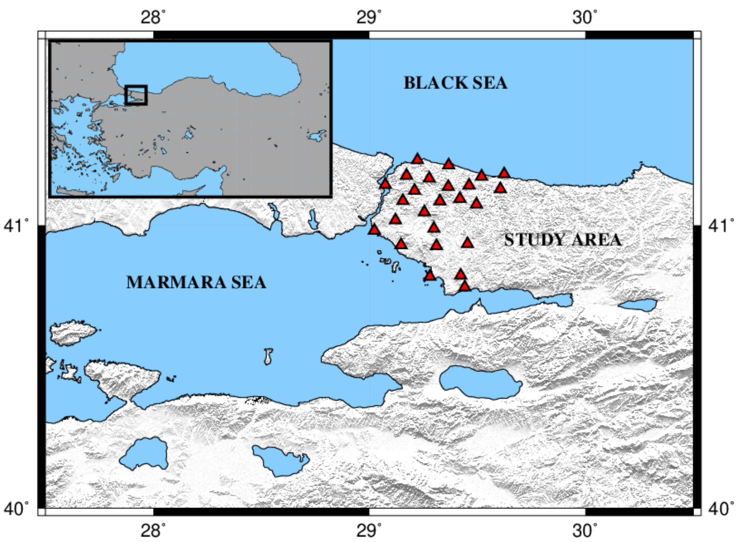

Figure 2. The area of interest (the red colored triangles represent the points in ITRF96 datum)

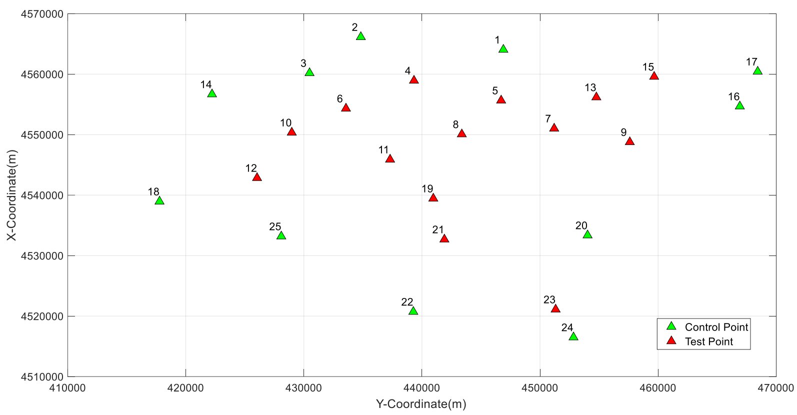

Figure 3. Distribution of the control (green colored triangle) and test (red colored triangle) points in area of interest

The distribution of control and test points is represented in Figure 3, where the green colored triangles show the control points, a total number of 11 and red colored triangles indicate the locations of the test points, a total number of 14. The representative figure has been drawn using ITRF96 datum coordinates of the points. The control points have been used to estimate the transformation parameters by changing the locations and numbers of them in each case. While increasing the number of the points in each case, the locations of the points are considered to cover the study area homogeneously. The test points have been used to check the validation of the estimated parameters that they are whether close to the original coordinates or not. The 14-test points have been converted to the second datum by using the transformation parameters estimated in each case and the obtained coordinates are compared with the original coordinates of the test points.

In the transformation problem, it is important that the common points in both datum should surround the area of interest to represent the region as a frame in terms of estimating the accurate transformation parameters. For this reason, this effect was considered in this study when the number of common points (here, control points) has been increased one by one, the distribution of the control points have been applied as surrounding the test points homogeneously. As mentioned, the 2D transformation parameters have been determined by increasing the number of control points that starts from 3 points, which is the minimum requirement for adjustment and up to 11 points. The name of the control points used in each case can be seen in Table 1.

Table 1 Definition of the cases with control points

Case	# Control Points	Control Points
1	3	17-14-24
2	4	17-2-18-24
3	5	17-2-18-24-25
4	6	17-2-18-24-25-1
5	7	17-2-18-24-25-1-14
6	8	17-2-18-24-25-1-14-20
7	9	17-2-18-24-25-1-14-20-3
8	10	17-2-18-24-25-1-14-20-3-22
9	11	17-2-18-24-25-1-14-20-3-22-16

In each parameter estimation case, the test points have been transferred to the other datum by using the estimated parameters and the coordinates of the test points transferred have been compared with the original datum coordinates. The four transformation parameters (two translation terms, one rotation component and one scale factor) are denoted as tx, ty, ε and k, respectively in 2D network (seen in Tables 2). Table 2 shows the 2D

International Journal of Engineering and Geosciences (IJEG),
Vol; 4, Issue; 2, pp. 058-062, June, 2019, ,

network solutions consisting of several scenarios. The cases are formed to detect the spatial and quantity relations between translation terms and rotation component, also to obtain the reliability of the results of the LS method. In Table 2, the transformation parameters are estimated for transferring coordinates from ITRF96 to ED50 datum.

Table 2 Estimated transformation parameters

# Case	t_x (m)	t_y (m)	k	ε (°)
1	174.0549509	44.5675821	1.0000024	359.9998570
2	175.5153203	45.1053020	1.0000020	359.9998526
3	175.7280878	46.2908093	1.0000020	359.9998382
4	174.9094627	46.5868773	1.0000021	359.9998335
5	174.2245164	47.0875161	1.0000023	359.9998263
6	176.8750128	47.0830701	1.0000017	359.9998294
7	175.6652566	47.8693917	1.0000020	359.9998180
8	177.5116814	45.3846153	1.0000016	359.9998511
9	177.2992547	45.9525747	1.0000016	359.9998438

Table 3 Coordinate differences between estimated and original test points in ED50 datum

	Case 1		Case 2		Case 3	
# Test Point	Δx (mm)	Δy (mm)	Δx (mm)	Δy (mm)	Δx (mm)	Δy (mm)
4	-28.1075	-32.4222	-26.9873	11.9954	-34.7223	17.0079
5	-38.4552	-26.7569	-35.6952	15.4949	-41.3323	20.7975
6	-9.4101	-29.5503	-7.2204	17.1075	-16.0715	23.7010
7	-41.2389	0.4561	-36.6152	41.5932	-40.7839	47.7386
8	-43.0124	-18.6888	-38.6761	25.0825	-44.7461	32.0361
10	0.7316	-16.5026	3.8706	31.9622	-5.8478	39.8899
11	-28.0566	-17.6561	-22.8189	28.4243	-30.1158	36.8710
12	2.6158	-30.7370	7.9874	19.2663	-1.9268	29.2988
13	-34.0988	-22.9626	-30.8915	16.6088	-34.5350	21.1942
19	-41.1820	2.0933	-33.5535	47.4689	-39.4601	57.2730
21	-36.8647	-2.8020	-26.9486	42.7850	-32.1274	54.2256
9	-72.5805	16.2343	-66.7297	55.4463	-69.1214	61.6929
15	-36.8233	-8.8609	-34.3552	28.8465	-37.0126	32.2189
23	-25.7702	23.3955	-11.3413	66.7847	-13.3056	80.4574
	Case 4		Case 5		Case 6	
4	-26.3673	14.7037	-26.2198	7.7581	-22.6288	-4.5261
5	-32.9398	20.0433	-32.3256	14.5271	-27.2439	-2.1807
6	-8.9904	20.7765	-10.1990	13.6096	-3.6433	4.3923
7	-32.8274	48.1446	-32.2950	43.8276	-24.7846	24.2868
8	-37.5976	31.1636	-38.1719	25.8840	-29.6930	10.7925
10	0.1671	36.4959	-2.1628	29.1899	6.9255	22.3993
11	-24.1907	35.2878	-26.0994	29.6888	-14.8919	17.8681
12	2.5443	26.0113	-1.1900	19.2344	12.3755	13.7329
13	-25.3895	21.7959	-23.6980	17.3296	-19.3497	-3.9899
19	-34.3520	56.8543	-36.6953	52.5648	-21.9766	38.2914
21	-28.1160	54.5255	-31.2778	51.2092	-12.7164	36.0325
9	-61.0287	63.3947	-60.0087	60.2435	-51.5488	36.8964
15	-26.8745	33.3903	-24.1022	29.1765	-21.9751	5.2229
23	-10.5283	83.3428	-14.1162	82.7720	10.6000	61.5524
	Case 7		Case 8		Case 9	
4	-17.0197	-17.3251	-13.9011	-22.0265	-10.9672	-24.0004
5	-20.9764	-12.5004	-20.9778	-21.6699	-17.2106	-22.9654
6	-0.3229	-8.9130	7.7319	-14.2711	9.7654	-15.8535
7	-18.7709	16.0019	-19.7481	2.5866	-15.5662	2.0434
8	-25.4725	0.7623	-21.5998	-10.4763	-18.4553	-11.1699
10	8.3494	8.7499	20.4395	2.6969	21.7455	1.4646
11	-12.9137	7.1665	-4.0771	-4.3656	-1.8579	-4.7350
12	11.3567	0.8505	27.7628	-8.5126	28.4295	-8.8839
13	-11.3476	-12.4187	-16.1882	-24.0984	-11.3677	-25.1796
19	-20.8637	29.7786	-11.8948	13.2482	-9.4303	13.8336
21	-13.0905	29.0990	-2.3043	8.3337	0.0446	9.8203
9	-44.8160	30.6438	-48.7086	13.6968	-43.7830	13.6656
15	-12.1562	-2.6723	-21.0110	-14.0933	-15.4434	-15.4407
23	9.2379	59.2548	18.6188	28.5184	21.7735	31.8196

To investigate the effect of the number of the control points used in the transformation problem, 9 different cases have been realized. In each case, the number of the control points has been increased one by one starting from 3 to 11. Table 3 shows the coordinate differences of the test points, which are obtained by subtracting the original coordinates from transformed coordinates. In addition to these results, to figure out the importance of the number of the control points to be used in transformation problem, the sum of the absolute differences of the coordinate components has been taken into consideration. When the number of the control points has been increased, a significant and clear improvement has been detected in the results. Table 4 shows this situation case by case in terms of the sum of absolute coordinate differences subtracted from original test points coordinates in ED50 datum and estimated coordinates of test points in ED50 datum. According to the Table 4, since from 3 to 7 reference points (Cases 1-5) provide similar results, the similar trend in results also is provided for the number of points from 8 to 11. However, a significant difference has been detected when the number of reference points is increased to 8. As can be seen from Table 4, although Case 1 provides a lower value than Case 2, the increase in Case 2 is not seen as a meaningful improvement. Contrary to this, after Case 6, a continuous decrease has been tracked.

Table 4. The sum of the absolute coordinate differences of test points between original and estimated ED50 datum coordinates.

The sum of the absolute coordinate differences $\|\Delta x\|+\|\Delta y\|$ (m)		
Case 1	Case 2	Case 3
0.6881	0.8326	0.9955
Case 4	Case 5	Case 6
0.8978	0.8356	0.5625
Case 7	Case 8	Case 9
0.4628	0.4436	0.4267

4. CONCLUSION

In this study, the basic geodetic application, so-called coordinate transformation problem has been examined with Helmert Transformation by increasing the quantity of the control points to achieve reliable accuracy for solving the datum transformation. The problem is tested by a network that includes 25 points with known coordinates in two different datum. 11 points have been used as control points to estimate the transformation parameters in defined cases in which the number of control points starts with 3 points and ends when reached to 11 points. The 14 points in this network have been used as test points, where the coordinates of them have been compared with transformed coordinates computed from the estimated parameters.

As mentioned before, for 2D coordinate transformation problem, minimum 3 common points should be known to estimate the transformation parameters as adjusted. However, the distribution and number of these common points should also be taken into account to obtain accurate transformation parameters. In this study, it is seen that the number of the common points affects the reliability of the results of the transformation problems, meanwhile the accuracy of the coordinates calculated by using these parameters. For this study area, the homogeneously distributed 8 common points provide reliable and accurate results to solve the transformation problem.

REFERENCES

Akyilmaz, O. (2007). Total Least Squares Solution of Coordinate Transformation. Survey Review, 39 (303), 68-80

Chen, W. and Hill, C. (2005). Evaluation Procedure for Coordinate Transformation. J. Surv. Eng., 131 (2), 43-49

Koch, K.R. (1999). Parameter Estimation in Linear Models. In: Parameter Estimation and Hypothesis Testing in Linear Models. Springer, Berlin, Heidelberg

Kutoglu, H.S. and Ayan, T. (2006). The role of common point distribution in obtaining reliable parameters for coordinate transformation, Applied Mathematics and Computation, 176, 751–758

Kutoglu, H.S. and Vaníček, P. (2006). Effect of Common Point Selection on Coordinate Transformation Parameter Determination, Stud. Geophys. Geod., 50, 525−536

Tan, Q., Lu, N., Dong, M., Zhu, L. (2013). Influence of geometrical distribution of common points on the accuracy of coordinate transformation, Applied Mathematics and Computation 221, 411–423

International Journal of Engineering and Geosciences (IJEG),
Vol; 4, Issue; 2, pp. 063-070, June, 2019, ISSN 2548-0960, Turkey,
DOI: 10.26833/ijeg.443114

DETECTION OF ECOLOGICAL NETWORKS AND CONNECTIVITY WITH ANALYZING THEIR EFFECTS ON SUSTAINABLE URBAN DEVELOPMENT

Serdar Selim[1], Nuster Demir *[1]

[1] Akdeniz University, Faculty of Science, Department of Space Science and Technologies, 07070, Antalya/TURKEY e-mail: (serdarselim/nusretdemir@akdeniz.edu.tr)

ORCID 0000-0002-5631-6253; ORCID 0000-0002-8756-7127

*Corresponding Author, Received: 12/07/2018, Accepted: 11/09/2018

ABSTRACT: Rapid urbanization is a leading process for the global environmental problems such as climate change, massive loss of natural habitats, an increase of air, water, soil quality and social troubles. Within the scope of elimination of these effects, detecting, preserving and managing a strategically planned ecological network can provide ecological, economic, social and cultural benefits. Specially, connectivity of landscape patches in urban areas is an important factor for urban ecosystem cycle. Ecological studies under these circumstances are concentrated in urban areas and strategies are being developed to create green systems by establishing links between green areas. In this study, a method based on the graph theory has been proposed to create ecological links between important landscape patches in the Chennai City and the effects of the created system on the city has been discussed. Firstly, a comprehensive database is created for Chennai in the GIS. And then, important urban landscape patches and connectivity are detected with use of Conefor software that enhances the quality of landscape patches and ensures that landscape connectivity is sustainable. With this scope, we used integral index of connectivity (IIC) index and the probability of connectivity (PC) index that have been known to show an enhanced performance for urban habitat conservation planning and change monitoring applications. Ultimately, the resulting findings are mapped in the GIS environment, and the ecological, social and cultural impacts of the system are discussed based on international literature.

Keywords: *Urban ecology, Landscape connectivity, Green infrastructure, GIS*

International Journal of Engineering and Geosciences (IJEG),
Vol; 4, Issue; 2, pp. 063-070, June, 2019,

1. INTRODUCTION

Along with the rapid urbanization and land cover changes in recent years, natural habitats became reduced in size and fragmented especially in developed and developing countries (Williams et al., 2009 and Hüse et al., 2016). The natural habitats are important for the citizens as well (Şimsek et al., 2018) and GIS methods are useful to determine the spatial problems (Akar et.al, 2018; Memduhoglu and Basaraner, 2018). Habitat fragmentation and division of landscapes, reduce the connectivity between habitat patches by extending the distances between the remaining habitat stands, which lead to the loss of biodiversity in the long process (Bogyó et al., 2015 and Hüse et al., 2016). Thus preserving biodiversity and sustainability of landscape special in urban areas have a high priority in urban ecological planning (Talley et al., 2007 and Zipkin et al., 2009). Habitat connectivity is the most necessary and important factor that promotes the preservation of biodiversity in degraded landscapes by promoting gene flow and the expansion of individuals movement areas between populations (Lindborg et al., 2012 and Hüse et al., 2016). Besides, these habitat connections also support the socio-cultural life in the city and increase the quality of life. In this context, especially in urban settlements, the evaluation of qualities of habitat patches and the determination of habitat connections are an important guide for future urban planning studies.

In a rapidly developing country such as India, the determination of the ecological characteristics of urban habitats is necessary for the future of Indian cities. As known, green spaces planning and accordingly management in urban areas up to now requires greater insights in socio-economical, socio-cultural, and ecological aspects that ensure a sustainable urban structure (Thompson, 2002; Govindarajulu, 2014). In this context, it is necessary to have information about the ecological structure of the Chennai City in India, which has entered into a process of rapid economic and cultural development, and to use this knowledge for the ecological development of the city. To reach mentioned targets above, the main target of the study is to detect the important landscape patches and connection of landscapes of Chennai city. This framework includes the detection of spatial elements (patch areas and sizes, ecological corridors, landscape matrix, etc.) (Govindarajulu, 2014). It is really important to connect the habitat patches (open green spaces such as parks, city garden, and urban forest) using corridors (green ways, river, and sides, tree-line roads etc.) to sustain ecological connectivity between landscape patches in landscape matrix. Landscape corridors are the most important parts of green space planning and management; and these corridors can be used to reduce the negative impact of landscape degradation (Majka et al., 2007). These corridors also support urban life and create interconnected open- green space systems called green infrastructure.

In generally, connectivity indexes have been used for determination of ecological connectivity. These connectivity indexes give accurate results quickly as integrated into the GIS software. It transformed and systematized the landscape structure that is complex and interactive, helping to describes the significance of every green space, and guiding urban and environmental planning for conservation of biodiversity and sustainable ecological development (Kong et al., 2010). In this study, Conefor Sensinode 2.2 software that can calculate the landscape connection has been used. Conefor software is known to exhibit a more advanced performance compared to other existing indexes with the new index (integral index of connectivity 'IIC', the probability of connectivity 'PC'). (Saura and Pascual-Hortal 2007, Saura and Rubio 2010, Saura et al., 2011). These indices are based upon mathematical graphs theory and measure the connections between habitat patches. These indices allow the assessment of linkages, connectivity, and availability of a habitat patch to other habitat patches. Thus, the landscape link is designed as a feature that determines and measures the number of patches available in a landscape matrix. The links do not assess whether the landscape patch is high or low quality, or whether it has strong ecological associations, but these links are an indication of whether the landscape patches are accessible (Saura and Torne, 2009).

This study, which was prepared to determine the habitat connections between selected landscape patches in the Chennai city and to provide ecological support to the city's future, will be an important data source for urban physical planning studies of the Chennai. Six landscape patches that affect the economic, cultural, social and ecological aspects of the city are selected and the connections between them are determined with help of remote sensing (RS) and geographical information systems (GIS). Then, these connections were evaluated based on landscape ecology and interpreted on the basis of landscape ecology to ensure sustainable urban development. Based on these results, we emphasize which patches are more important to the city.

2. MATERIALS AND METHODS

2.1 Study area

The second level headings should be in 10pt, bold, justified, and capitalized font. Leave one blank line both before and after the heading, respectively. Chennai is among the top five cities and is the capital of the Indian state of Tamil Nadu (N 13° 5′ 0″, E 80° 16′ 0″). It is located on the Coromandel Coast off the Bay of Bengal, it is one of the most important centers of the economy, education and culture in South India. Chennai has a flat and wide area in this context it expanded from 174 km2 to an area of 426 km2 dividing into three regions (North, South, and Central) which covers 200 wards in 2011 (Wikipedia, 2016). The climate of that region is tropical wet and dry. Maximum temperatures are around 35-40 ºC, minimum temperatures are around 19-25 ºC (IMD, 2010). Chennai shows a similar process of urbanization as in other major cities: increasing land use intensity and intensive pressure on natural areas (Fig 1).

International Journal of Engineering and Geosciences (IJEG),
Vol; 4, Issue; 2, pp. 063-070, June, 2019,

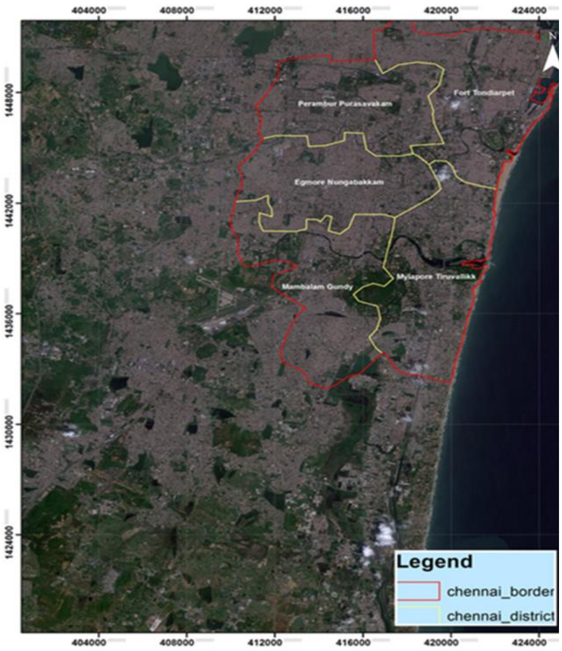

Figure 1. Location of study area

According to the official records of the year 2011, the city is home to 4,646,732 inhabitants (MUB, 2011). Chennai is one of the most visited cities in India because it has many historical and cultural riches, especially UNESCO's Mahabalipuram Heritage Site. In this context, the city visited more than 3 million tourists in 2011. Three long rivers and many lakes spread across the city attract ecologically interested tourists. (Wikipedia, 2016). These wetlands have unique ecology and endemic flora and fauna (Zanakiraman et al., 2013). A considerable part of the urban wetlands is thought to have been transformed, especially for agriculture and settlement. Since the beginning of the 20th century, the amount of wetlands in the Chennai has decreased from 150 to under 30 currently. The important wetlands include Ennore creek, Adyar Estuary, Korattur swamp, Adambakkam Ambattur and Chitlapakkam lakes, Madhavaram and Manali Jheels, Pulicat and Vyasarpadi lakes, Coovum and Otteri nullah, and Buckingham Canal. (Gubta and Nair, 2011; The Economist, 2015). The region has an important area ecologically. For the sustainability of the region, ecological characteristics must be preserved and maintained in the Chennai.

2.2. Data

In the study, six regions were selected which are important in terms of their ecological characteristics, affecting the city of Chennai ecologically, economically, socially and culturally (Fig 2).

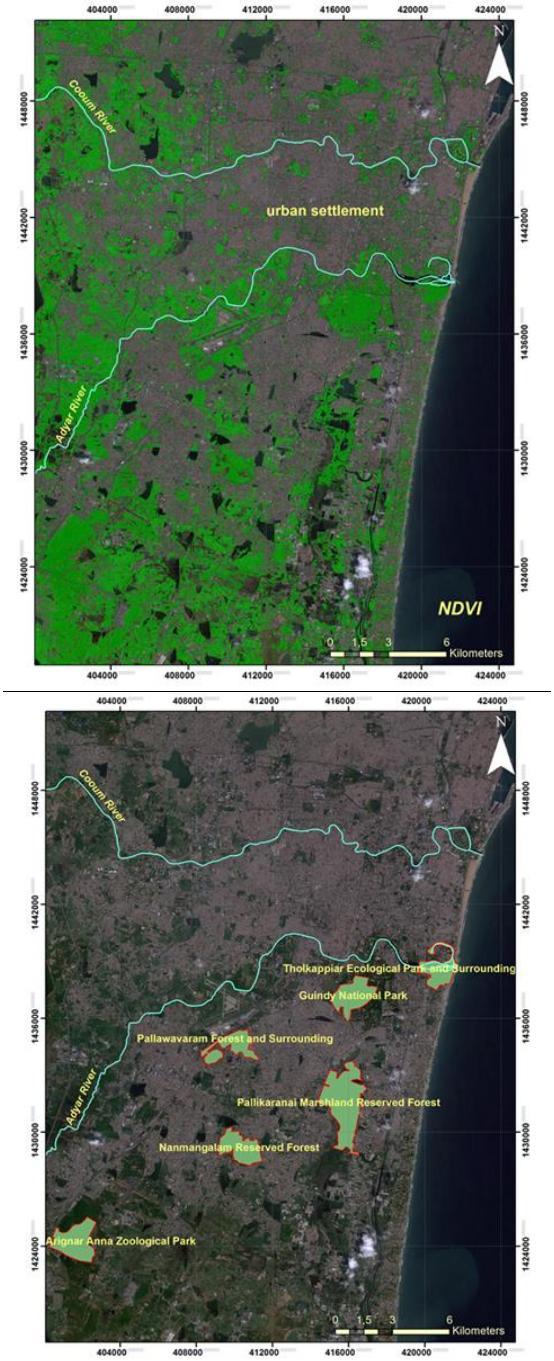

Figure 2. Normalized Difference Vegetation Index of Chennai Around, Selected ecological areas (right)

(1) Guindy National Park, it is the 8th smallest National Park of India, is a protected area of Tamil Nadu, located in Chennai, and one of the rare national city parks. There are more than 350 species of plants, including many trees, shrubs and ground cover plants, and there are wetlands and pastures. There are also 24 varieties of trees. There are over 14 species of mammals and over 150 species of birds (Oppili, P., 2004). (2) Tholkappiar Ecological Park (also known as Adyar Poonga or Tholkappia Poonga) set up by the Government of Tamil Nadu in the Adyar estuary area of Chennai, India. About 50 percent of the park is covered by water. A total of 143 species of fish, amphibians, birds, and reptiles have been

seen in the park (Lopez, 2011). (3) The Arignar Anna Zoological Park is located at Vandalur in the south-western part of the Chennai Metropolitan Area known as the Vandalur Zoo that is located within an open green area of more than 500 hectares). (Urban Green Belt, 2016). The zoo is located within the Vandalur Reserve Forest area. The zoo's ecosystem consists of dry deciduous and dry evergreen scrub forest vegetation of the Eastern Ghats (Wikipedia, 2016). (4) Pallikaranai Marshland Reserved Forest, one of the last remaining natural wetlands in the city collects flood water and increases ground water levels in landscape (Bhaskar et al.,, 2011). An extensive low-lying area covered by a mosaic of aquatic grass species, scrub, marsh, and water-logged depressions. (5) Nanmangalam Reserved Forest is a protected area located in the southern part of Chennai, about 24 km from the city center. It is a scrubland and is home to some of the rare territorial orchids (Padmanabhan, 2016). (6) Pallavaram is a residential locality in Chennai and a selection-grade municipality located in the Metropolitan city of Chennai. The Pallavaram forest, surrounded by settlements, is isolated from other ecological areas. Although it is a small area, it contains aquatic and terrestrial plant and animal species.

Other research materials used in the study are written and visual documents about Chennai, Sentinel 2 satellite images dated 03.10.2016 and cloudiness % 0,001, ArcGIS 10.1, QGIS 2.18 and Conefor Sensinode 2.2 software's (Table 1).

Table 1. Sentinel 2 used bands and features

Sentinel-2 Bands	Wavelength	Resolution
Blue	0.490 μm	10 m
Green (	0.560 μm	10 m
Red	0.665 μm	10 m
NIR	0.842 μm	10 m

2.2. Method

The method has four main processing stages (1) A comprehensive database is created for Chennai in the GIS (Fig. 3). At this step, Sentinel II satellite images were downloaded, 4-3-2 band combinations were prepared and a base map was created. The ecological, social and cultural data of the research area have been obtained in the direction of literature and related institutions and organizations. (2) At this stage, large habitat patches that affect the city ecologically, socially and culturally have been identified and digitized. (3) At the end of the method, connectivity indices (especially IIC and PC) were used and analyzed to measure the quality and linkages of large habitat patches.

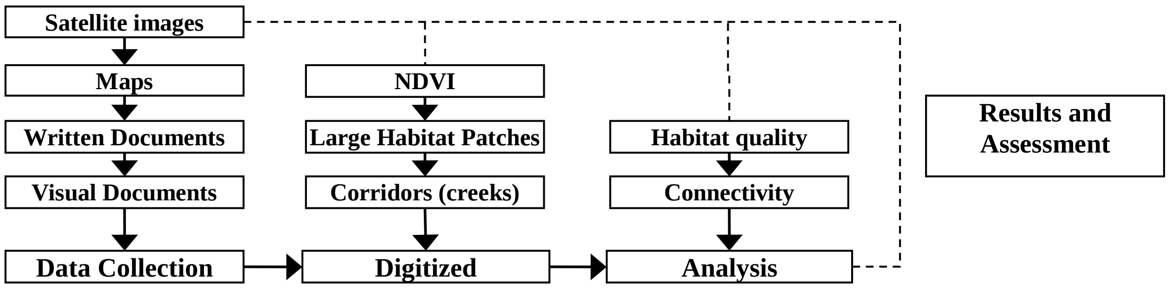

Figure 3. Method flowchart

After the analysis phase, four indices of Conefor software have been used to determine habitat quality and connectivity. These metrics are defined in Table 2. These indices are more preferred for landscape planning and conservation than other existing indices and these indices are important in defining critical habitat patches and landscape connectivity (Saura and Pascual-Hortal 2007) as shown in Table 2.

Table 2. Metrics and properties used in the study landscape changes (Saura and Pascual-Hortal 2007).

Index	Definition	Measuring
dA	This index will be used to analyze the extent to which the sequences provided by different topological indices differ from the priorities used to obtain basic patch characteristics such as habitat area and habitat quality. (Baranyi et all, 2011)	Values close to each other may show similar patches, especially in the shape area. When the area of a habitat patch increases, the quality also increases relatively.
BC	This index is used to assess the frequency with which shortest paths can be used along with a given patch, to determine how much a patch contains the current flow of the organism. (Baranyi et all, 2011)	The shortest paths between all pairs of patches are summed to calculate how many patches exist between all pairs of patches in a scene. The patches with high BC values are proposed to form the spine of the landscape. (Saura and Pascual-Hortal 2007).

dPC	This index is a graph-based habitat availability metric that quantifies functional connectivity (Saura and Pascual-Hortal 2007). A habitat availability (reachability) index taking into account varying probabilities of direct dispersal (pij) between different pairs of patches (Bodin and Saura, 2010)	PC ranges from 0 to 1 and increases with improved connectivity. When two patches are isolated from each other, PC=0; When two patches are completely connected to each other, PC=1.
dIIC	This index works similarly to the PC index, but instead of evaluating the probability of scattering across all pairs of patches, this metric uses the probabilities of distribution across all patches. (Bodin and Saura, 2010).	IIC ranges from 0 to 1 and increases with improved connectivity strength. If direct dispersal between any patches in the landscape is assessed as being possible, the link strength is set to unity. In other words, it is set to 0 (that is, the connection is not assigned between two patches).

In particular the PC and IIC indices, are used to comment the connectivity and quality of the determined landscape patches. These indices are calculated as shown in Figure 6. These connectivity indices enhance the quality of other frequently used indices for planning conservation applications of landscape, including their abilities both for adequately reacting to existing landscape changes and for determining the most important habitats for the sustainable of significant landscape connectivity (Pascual-Hortal and Saura 2006, Saura and Pascual-Hortal 2007, Saura and Torne, 2009).

$$PC = \frac{\sum_{i=1}^{n}\sum_{j=1}^{n} a_i \cdot a_j \cdot p_{ij}^{*}}{{A_L}^2} \qquad (1)$$

Where n is the number of patches in the current landscape. ai refers to each habitat area, the total landscape area is defined as AL. pij is the probability of a species moving directly from i to j (without passing by).The probability pij is calculated based on a negative exponential dispersal kernel.

$$IIC = \frac{\sum_{i=1}^{n}\sum_{j=1}^{n} \frac{a_i \cdot a_j}{1+nl_{ij}}}{A_L^2} \qquad (2)$$

Here, n is the total landscape patches number, ai and aj are the qualification of patch i and j, nlij is the shortest path links number between landscape patches i and j, and maximum landscape attribute defined as AL. IIC=1 means, habitats spread throughout all landscapes.

After the analysis phase, in order to the sustainability of the city, the determined habitats and linkages were assessed based on landscape ecology, using the numerical data obtained. In the assessment process, the importance of sensitive areas in terms of ecological characteristics was emphasized and supported with obtained data from analysis.

3. RESULTS

The first result is the areas and perimeter length of six landscape patches (Tholkappiar Ecological Park and Surrounding, Guindy National Park, Pallikaranai Marshland Reserved Forest, Pallawavaram Forest, and Surrounding, Nanmangalam Reserved Forest, Arignar Anna Zoological Park) (Table 3). The patch with ID 3 has a larger area than the others and therefore has a more ecological impact on the city. But it does not have a compact form, as seen from the perimeter length. In this case, it can be interpreted that the edge effects on the habitat patch are excessive (Forman, 1995). This may be advantageous for external species, creating a disadvantage for internal species. The patch with ID 2 has a partially compact form. Therefore, it is understood that habitat quality is not bad especially when compared to patch 4 (Table 3).

Table 3. Landscape patches and formal sizes

Name	Patch ID	Shape length (m)	Shape area (m^2)
Tholkappiar Ecological Park and Surrounding	1	11819,6	2420852,76
Guindy National Park	2	8485,57	2999596,45
Pallikaranai Marshland Reserved Forest	3	17725,88	6368998,11
Pallawavaram Forest and Surrounding	4	12567,68	2461131,42
Nanmangalam Reserved Forest	5	8653,67	2739789,50
Arignar Anna Zoological Park	6	8837,76	3392412,95

The length of the shortest distances between landscape patches is important in terms of connectivity. The shortest distances of each patch with other patches were determined (Table 4). It is understood that land uses between patches are mostly settlement. All patches are surrounded by settlements. So the patches are under concrete pressure and need to be protected. To ensure the sustainability of these patches, buffer zones must be

International Journal of Engineering and Geosciences (IJEG),
Vol; 4, Issue; 2, pp. 063-070, June, 2019,

created in the impact zone and the pressure must be reduced. Urban eco-zones protect fragmented landscape patches. When the ecological characteristics of the city are taken into consideration, it is clear that the necessity of protecting these landscape patches in the city is obvious (Fig 4). The distances between patches are listed in Table 4.

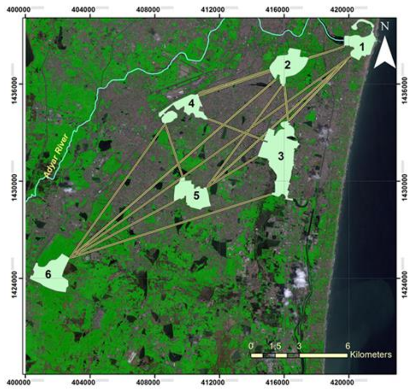

Figure 4. Detected patches and their numbers

Table 4. Shortest distances between the patches

From	To	Distance(m)	From	To	Distance(m)
1	2	2289.90	2	6	16852.90
1	3	5539.84	3	4	3675.99
1	4	9453.78	3	5	3678.35
1	5	12050.45	3	6	13042.51
1	6	21395.89	4	5	3441.35
2	3	2727.25	4	6	10139.66
2	4	4326.38	5	6	7327.02
2	5	7801.14			

4. DISCUSSION

Patches 2, 3, 4 and 5 are spread between 1 and 6 patches, and close to each other. The connections between internal patches (id; 2, 3, 4, 5) are short and more influenced by each other ecologically. The longest distance is approximately 21 km from the patches 1 and 6. The shortest distance is 2127.25 m from the patches 2 and 3. The distance between patches is used to interpret the connections of the complex landscape structure. Chennai city has a complex landscape structure. Connectivity analyses of the patches are calculated with the metrics used in the evaluation of complex landscapes (Table 5). Using Conefor Software, it tried to understand landscape ecology with graph theory. The graph theory and the used algorithms show that it is a powerful and effective way to represent landscape structure to make a complex analysis of functionally interconnected patches (Pascual-Hortal and Saura 2006, Pascual-Hortal and Saura 2008).

Table 5. The results of connectivity and quality analysis for selected landscape patches

Node	dA	BC	dPC	dIIC
1	11.87	0.00	0.20	0.19
2	14.71	0.03	0.29	0.25
3	31.24	0.03	0.56	0.53
4	12.07	0.23	0.22	0.22
5	13.44	0.10	0.26	0.23
6	16.64	0.00	0.23	0.24

As regards the dA value of all landscaping patches is assessed, it is seen that patch 3 is different from the others. This difference is the size of the patch. As the landscape patches in the city, it develops ecologically (Forman, 1995). Patch 1 is partly smaller and fed by Adyar River. Adyar River is a natural ecological corridor and positively affects the ecological structure of the route it passes through. It positively increases the ecological characteristics of the city and patch 1 because it is adjacent to the sea.

When BC value is assessed; In particular, patch 4, is the backbone of the landscape due to the number of connections. 2, 3 and 5 patches also contribute to urban ecology by providing connections between the determined landscapes. The important point here is the existence of landscape patches due to the city's ecological and socio-cultural structure. This interim patches, improve ecological circulation in the city and provide a positive impact on the city. In particular, these internal patches can be interconnected by rearranging urban ecological corridors (linear items such as main streets and boulevards, etc.) and stimulate urban ecological and cultural life.

The difference of the IIC metric from the similar PC metric is based on networks with weightless connections (Bodin and Saura, 2010).

The combination of PC and IIC metrics is assessed together because it shows the connection requirements of a particular patch and its sensitivity to interruptions and also created corridors are not weighted. IIC is sensitive to the changes in habitat, it helps to understand the connectivity between the landscape elements. On the other hand, PC is more probabilistic, and uses weights, except with these criteria, it is similar to the IIC metric (Gergel and Turner, 2017). The two metrics allows to see how the areas separated and isolation effects (Neel et al., 2014).

In the study, patch 3 is significantly different from the others according to PC and IIC values. It almost got 2 times more points than others. When the ecological characteristics of the city are assessed on the basis of the connection, it is seen that the most important patch is 3 (Pallikaranai Marshland Reserved Forest) for the city. Patches according to importance ratings are listed as 2, 5, 6, 4 and 1. Therefore, this ranking should be taken into account in conservation studies of the Chennai City.

5. CONCLUSION

Natural and semi-natural habitats have been dramatically reduced in the region as a result of the distorted urban extension. Despite the negative changes the remnant semi-natural habitat patches still harbor important diversity. It is very important to protect and improve the habitats of this biological diversity. In this study, the ecological connections of important landscapes are defined to protect and improve habitat life in the city. The provision of the connections between the patches is expected to improve the ecological and cultural life of the city.

Saura and Rubio stated in 2010 that the ranking obtained from the connectivity analysis is effective in preserving landscapes patches. Bodin and Saura stated in 2010 that IIC, PC and BC metrics jointly assess both the immediate connectivity impacts of the loss of a particular patch and the resulting increased vulnerability of the network to subsequent disruptions. In this study, the integration of different metrics was achieved using a network-based approach while assessing the importance of landscape patches. As we have shown in the study, the multifunctional connectivity can help a related researcher to assess different connectivity aspects of individual patches in an integrated way without being limited to either one of these conceptual assessments. As Baranyi et al., pointed out in 2011, these methods purpose to indicate and rank the relative contribution of landscape patches to the maintenance of connectivity, it is importance to gain a clear understanding their relationships and practical differences for the analysis of fragmented landscape networks. Findings from the study will provide a better understanding of the relationships between landscape patches and it will also contribute to ecological research and applications on the region by revealing the connections and relations between landscape patches.

REFERENCES

Akar, A , Gökalp, E. (2018). Designing A Sustainable Rangeland Information System For Turkey. International Journal of Engineering and Geosciences 3 (3), 87-97. DOI: 10.26833/ijeg.412222.

Baranyi, G., Saura, S., Podani, J., Jordan, F. (2011). Contribution of habitat patches to network connectivity: Redundancy and uniqueness of topological indices, Ecological Indicators 11, 1301–1310.

Bhaskar, A., Rao, G.B., Vencatesan, J. (2011). Characterization and Management Concerns of Water resources around Pallikaranai Marsh, South Chennai. A Volume in the Advances in Environmental Engineering and Green Technologies Book Series. Chapter 7, 102-121.

Bodin, Ö., Saura, S. (2010). Ranking individual habitat patches as connectivity providers: Integrating network analysis and patch removal experiments. Ecological Modelling 221,2393–2405.

Bogyó, D., Magura, T., Simon, E., Tothmeresz, B. (2015) Millipede (Diplopoda) assemblages alter drastically by urbanisation. Landscape and Urban Planning133, 118–126.

Forman, R.T.T. (1995). Land Mosaics, The Ecology of Landscape and Regions, Cambridge University Press, Cambridge, UK, 656p.

Gergel, S.E., Turner, M.G. (2017). Learning Landscape Ecology: A Practical Guide to Concepts and Techniques,Springer, 340 p.

Gubta, A.K., Nair, S.S. (2011) Urban floods in Bangalore and Chennai: risk management challenges and lessons for sustainable urban ecology. Current Science 100(11),1638-1645.

Govindarajulu, D. (2014). Urban green space planning for the climate adaptation in Indian cities, Urban Climate, 10(1), 35-41.

Hüse, B., Szabo, S., Deak, B., Tothmeresz, B. (2016). Mapping an ecological network of green habitat patches and their role in maintaining urban biodiversity in and around Debrecen city (Eastern Hungary). Land Use Policy 57, 574-581

IMD (2010). Indian Meteorological Department, Ever Recorded Maximum Temperature, Minimum Temperature and 24 Hours Heaviest Rainfall up to 2010, 67p.

Janakiraman, A., Naveed, M. S., Muthupriya, P., Sugumaran, J., Sheriff, M. A., Altaff, K. (2013). Studies on the zooplankton biodiversity and density in Adyar estuary, Chennai, India. Journal of Environmental Biology 34(2) ,273-275.

Kong, F., Yin, H., Nakagoshi, N., Zong, Y. (2010). Urban green space network development for biodiversity conservation: identification based on graph theory and gravity modeling. Landscape and Urban Planning 95 (1–2), 16–27.

Kuşçu Şimşek, Ç , Türk, T , Ödül, H , Çelik, M. (2018). Detection Of Paragliding Fields by GIS. International Journal of Engineering and Geosciences 3 (3), 119-125. DOI: 10.26833/ijeg.413833

Lopez, A,X. (2011). More winged visitors flock to Adyar Poonga. The Hindu, Online edition of India's National Newspaper.

Majka, D., Jenness, J., Beier, P. (2007). Corridor Designer: ArcGIS tools for designing and evaluating corridors. http://corridordesign.org/downloads (Access date: 04.01.2017).

Memduhoglu, A , Basaraner, M . (2018). Possible Contributions of Spatial Semantic Methods And Technologies to Multi-Representation Spatial Database Paradigm. International Journal of Engineering and Geosciences 3 (3), 108-118. DOI: 10.26833/ijeg.413473.

MUB (2011). Ministry of Urban Development, Government of India. India Smart City Profile report, 5p.

Neel, M., Tumas, H. R., & Marsden, B. W. (2014). Representing connectivity: quantifying effective habitat availability based on area and connectivity for conservation status assessment and recovery. PeerJ, 2,e622.doi.org/10.7717/peerj.622

Oppili, P. (2004). Looking for exotic species at the Guindy National Park. The Hindu, Online edition of India's National Newspaper.

Padmanabhan, G. (2016). Chennai's eco spots. The Hindu, Online edition of India's National Newspaper.

Pascual-Hortal, L. and Saura, S. (2006). Comparison and development of new graph-based landscape connectivity indices: towards the priorization of habitat patches and corridors for conservation. Landscape Ecology 21 (7), 959-967.

Pascual-Hortal, L. and Saura, S. (2008). Integrating landscape connectivity in broad-scale forest planning through a new graph-based habitat availability methodology: application to capercaillie (Tetrao urogallus) in Catalonia (NE Spain). European Journal of Forest Research 127, 23-31.

Saura, S., Estreguil, C., Mouton, C., Rodríguez-Freire, M. (2011). Network analysis to assess landscape connectivity trends: application to European forests (1990-2000), Ecological Indicators 11, 407-416.

Saura, S., Pascual-Hortal, L. (2007). A new habitat availability index to integrate connectivity in landscape conservation planning: comparison with existing indices and application to a case study. Landscape Urban Plan. doi:10.1016/j.landurbplan.2007.03.005.

Saura, S., Rubio, L. (2010). A common currency for the different ways in which patches and links can contribute to habitat availability and connectivity in the landscape". Ecography 33, 523-537.

Saura, S., Torné, J. (2009). Conefor Sensinode 2.2: a software package for quantifying the importance of habitat patches for landscape connectivity. Environmental Modelling & Software 24,135-139.

Talley, T.S., Fleishman, E., Holyoak, M., Murphy, D.D., Ballard, A. (2007). Rethinking a rare-species conservation strategy in an urban landscape: the case study of a valley elderberry longhorn beetle. Journal of Biological Conservation 135, 21–32.

The Economist (2015). Next time by water. Flood and India's Coromandel Coast, http://www.economist.com/news/asia/21679822-floods-should-be-warning-those-building-state-capital-scratch-next-time-water. (access date: 02.01.2017).

Thompson, C.W. (2002). Urban open space in the 21st century, Landscape Urban Planning., 60 (1), 59–72.

Urban Green Belt, (2016). http://edugreen.teri.res.in/explore/forestry/urban.htm (access date: 10.07.2018).

Wikipedia, (2016). Chennai. https://en.wikipedia.org/wiki/Chennai (access date: 04.01.2017)

Williams, N.S.G., Schwartz, M.W., Vesk, P.A., McCarthy, M.A., Hahs, A.K., Clemants, S.E., Corlett, R.T., Duncan, R.P., Norton, B.A., Thompson, K., McDonnell, M.J. (2009). A conceptual framework for predicting the effects of urban environments on floras. Journal of Ecology 97, 4–9.

Zipkin, E.F., DeWan, A., Royle, J.A. (2009). Impacts of forest fragmentation on species richness: a hierarchical approach to community modeling. Journal of Applied Ecology 46, 815–822.

International Journal of Engineering and Geosciences (IJEG),
Vol; 4, Issue; 2, pp. 071-077, June, 2019, ISSN 2548-0960, Turkey,
DOI: 10.26833/ijeg.450571

HUMAN RESOURCE MANAGEMENT USING GEOGRAPHIC INFORMATION SYSTEMS (GIS): AN EXAMPLE FROM TURKISH LAND REGISTRY DIRECTORATES

Fred Ernst[1]*, Saffet Erdoğan[1], Yüksel Bayram[2]

[1]Harran University, Engineering Faculty, Department of Geomatics Engineering, Şanlıurfa, Turkey
(f.b.ernst/serdogan@harran.edu.tr);
[2] General Directorate of Land Registry and Cadastre, Arsus, Turkey (yukselbayram73@hotmail.com)

ORCID 0000-0002-7568-2582; ORCID 0000-0003-2846-853X; ORCID 0000-0001-7686-8648;

*Corresponding Author, Received: 03/08/2018, Accepted: 23/10/2018

ABSTRACT: Recently, a new interest in the social science community in location and a new "spatial social science" that crosses the traditional boundaries between disciplines have emerged. In this context, we will examine the usage of Geographic Information Systems (GIS) in the analysis of human resource management in the public sector. For this research, personnel and operational data of 957 Land Registry Offices in all districts of Turkey were used. These operational data were examined using different clustering techniques. By using tools of Geographic Information Systems to analyze public services, the distribution and condition of services can be understood much better. This study shows the first step to improve them and to allow for making better-informed decisions on where, when and what kind of resources to allocate in the human resource management in the public sector.

Keywords: *Clustering, GIS, human resource management, spatial analysis*

1. INTRODUCTION

Until recently, for many social scientists, location was just another attribute in a table and not a very important one at that. This was based on the assumption that processes leading to social deprivation, crime, or family dysfunction are more or less the same everywhere. According to this belief, many other variables, such as education, unemployment, or age, are far more interesting as explanatory factors of social phenomena than geographic location.

Those who believe in such a paradigm forget that even in the 18th century the well-known economist Adam Smith addressed in his book “The wealth of nations” the issue that the physical geography of a region can influence its economic performance. For example, he contended that the economies of coastal regions, with their easy access to sea trade, usually outperform the economies of inland areas.

However, when Sachs et al. (2001) were trying to answer the similar question “Why are some countries stupendously rich and others horrendously poor?” they used Geographic Information Systems (GIS). Tomlinson who is called the “father of GIS” (Tomlinson et al. 1999, Tomlinson, 2011) defined GIS as a system that stores spatial data replete with its linked logically attribute information, in a GIS storage database, where analytical functions are controlled interactively by a human operator to generate the needed information products. GIS is a particularly horizontal technology in the sense that it has wide-ranging applications across the industrial and intellectual landscape.

As Michael Goodchild outlined in his essay “Social Sciences: Interest in GIS grows” (Goodchild, 2004), many social scientists have started to talk about a "spatial turn," which refers to the importance of location, and a new "spatial social science" that spans the traditional boundaries between disciplines. As a result, rising interest in GIS and what it makes possible: (mapping, spatial analysis, and spatial modeling) can be noticed. For example, in criminology, geographic profiling has been used for about 20 years (Harries et al., 1999). This tool for fighting crime makes use of the principle of distance decay, which is applied to the behavior of the offender and the locations of a series of crimes that show the same used methods. GIS generates distance decay surfaces centered on each crime and superimposes it to create a three-dimensional surface that likely peaks in the criminal's home area.

Especially, different kinds of clustering techniques have been proven to be useful in the analysis of complex and extensive socio-economic data (big data). According to Jan et al. (1999) clustering can be defined as “the unsupervised classification of patterns (observations, data items, or feature vectors) into groups (clusters)”.

The usage of Empirical Bayes smoothing approach is very common in population related studies. For example, Sparks et al. (2013) used this approach to the study of racial and poverty segregation and infant mortality rates in the US. They used both Exploratory Spatial Data Analysis methods and Hierarchical Bayesian spatial regression models to examine the influences of these segregation measures on the infant mortality rate for each county, net of income inequality, degree of rurality and relative socio-economic deprivation. Their spatial analysis of racial segregation suggested that when blacks live in close proximity to each other, this tends to increase the infant mortality rate.

Moran’s I index has been widely adopted in the GIS community and has become part of many GIS software packages. It is explained in detail in the standard GIS textbook “The ESRI Guide to GIS Analysis” (Mitchell, 2005) where some applications in the field of population science are given as well.

The Getis-Ord G* index was introduced by Getis et al. (1992) in 1992 and has become a standard tool for spatial statistics. The empirical work in their article included studies of sudden infant death syndrome by counties in North Carolina and dwelling unit prices in metropolitan San Diego by zip-code districts. Their results indicated that the Getis-Ord G* index should be used in conjunction with Moran’s I index in order to identify characteristics of patterns not revealed by the Moran’s I index alone.

Recently, many local governments have responded to the challenge of decreasing budgets by instituting performance management systems for their departments (Oliver 2005). Such systems enable governments to make decisions based on sound financial analysis and to target their limited resources toward productive programs. The systems gather various performance data as indicators of effectiveness and use trend analysis to inform officials and managers who allocate resources and make decisions. In addition, these systems can determine if programs are achieving the desired results and meeting the needs of the public.

In a recent research (İşcan et al. 2017), web sites of local governments in Turkey have been evaluated regarding city guides and applications for e-municipality. They stated that GIS is used by municipalities to provide better services and to improve decision making mechanisms including tax administration and city planning.

1.1 GIS for Human Resource Management as a new application in Turkey

In Turkey, GIS based studies are generally related to urban management applications (Çabuk, 2015), health applications (Demirel et al., 2009), traffic applications (Erdoğan, 2009), infrastructure applications (Furat et al. 2015), criminology applications (Erdoğan, 2013) and environmental research applications (Ernst, 1996). In the areas of social sciences and public service management, GIS applications are hardly used. Among these few studies Türk (2011) can be mentioned. He investigated the distribution of crimes in Turkey using GIS. He concluded that GIS based analysis might help to analyze existing social problems in Turkey and to provide criminologists and sociologists with new tools to tackle these problems.

In the domain of public service management, GIS can be utilized to visualize the geographic distribution of public services, to investigate the statistical increase or decrease in these services, to analyze and map ratios and trends in public service performance, and to locate problematic areas. GIS can also be deployed for temporal, spatial or time-space integrated clustering studies based on various sets of criteria. Within the scope of public management, human resource management refers to the complete set of human resources employed as public officials and employees providing public services for the community in state institutions and organizations. The concept of human resource management in public services can be examined under three main components: human resource planning, better employment of human resources and developing the efficiency and effectiveness of human resources by providing effective training (on-site or distance learning) (Yuluğ, 1971).

Human resource management is the main part of three components and is defined as employing an adequate number of highly-qualified public personnel with a proper distribution and appropriate timing with the aim of performing the provided and projected social services. In addition, human resource planning can be defined as predicting the short, medium and long-term needs of society and as considering the ratio between geographic, economic and socio-cultural features and providing a cost-effective public service. It covers the employment, management, and planning of the most fitting human resources for the public service. Human resource planning entails two key objectives, the first is enabling the most effective use of human resources in public institutions and the second is meeting the human resource needs of the institution in terms of both quantity and quality for future operations. The reasons necessitating human resource planning in public institutions are; the cost of human resources, social and political changes, advancements in science and technology, the inadequacy of public personnel with respect to quantity and quality, and the rapid increase of digital data (Dikmetaş et al., 2000).

The applicability and validity of planning necessitate not only the accessing of correct information at the correct time but also the utilization of the best-tailored analysis techniques. Therefore, the purpose of the present study is to detect underload and overload of human resources within the General Directorate of Land Registry and Cadastre–Turkey (TKGM) by applying different GIS based spatial analyses. For this, we have examined the total number of annual title transactions executed in its 957 Land Registry Offices that operate and provide public services. In addition, we examined the total number of personnel employed in the directorates of the land registry.

2. DATA AND METHODOLOGY

In this study, we collected figures for the total number of sales, nationalization, evacuation, incorporating, public works, donation, hypothecation, land use conversion, property ownership identification, construction servitude identification, and lifelong support agreement works received from baye for the period from 2013 to 2014 on the basis of land directorates within each single city and town (TSM). Other data include the number of personnel received from TSMs.

GIS based visualization of the geographic distribution of public services is a method that is useful in detecting the density of served areas. Visualization is the first stage of GIS analysis and a number of social and academic GIS studies in Turkey provide research information about this stage. In the second stage, using several exploratory-descriptive spatial statistical tools of GIS, it is possible to provide a statistics-assisted description of the current situation in public services and a description of the sectoral problems. Spatial analyses used at this stage can be categorized into two different groups: first order and second order analyses.

First order analyses investigate spatial changes in the data whilst second order analyses spatial covariance between the data. Thus, first order analyses aim to detect data changes in density analysis, spatial ratio analysis etc. and global and regional trends and outliers and second order analyses aim to estimate spatial dependency and changes in spatial dependency between the data. In the complete set of first and second order analyses, the aim is to better understand data structure and the spatial distribution of the data by computing various descriptive statistical indices. By detecting temporal and spatial clustering of the data, priority action areas are detected and confirmed. Exploratory/descriptive spatial statistical methods used at this stage are vital to the detection of the structure and distribution of public service-relevant data; their interactions with the environment; areas in which the services defined as hot or cold points are located and their density.

Although these methods are effective in detecting the outliers and trends in spatial data and various sets of clustering, they still fail to explain the underlying mechanisms of clustering. In the spatial modelling process, which is the third step in GIS assisted analyses, modelling studies are conducted on the basis of several explanatory independent variables and their spatial distribution. Using such spatial modelling methods, hypotheses related to the case study and factors affecting the distribution of a particular case can also be tested on the basis of spatial relations (Demirel et al., 2009)

GIS is a frequently applied method that is useful in detecting area density with respect to certain criteria and to visualize the geographic distribution of public services. In order to provide visual information, thematic maps that display personnel distribution in Land Registry Directorates and population/personnel ratio are devised in the first stage (Figure 1).

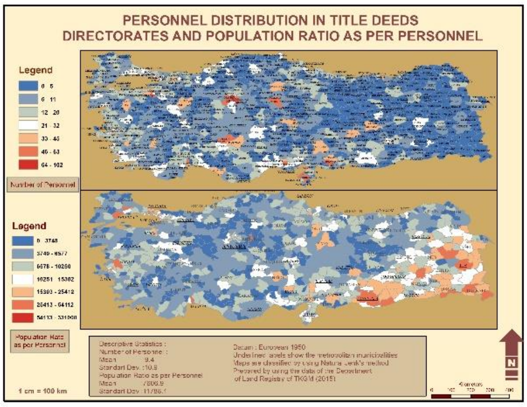

Figure 1: Personnel distribution in Land Directorates and population/personnel ratio.

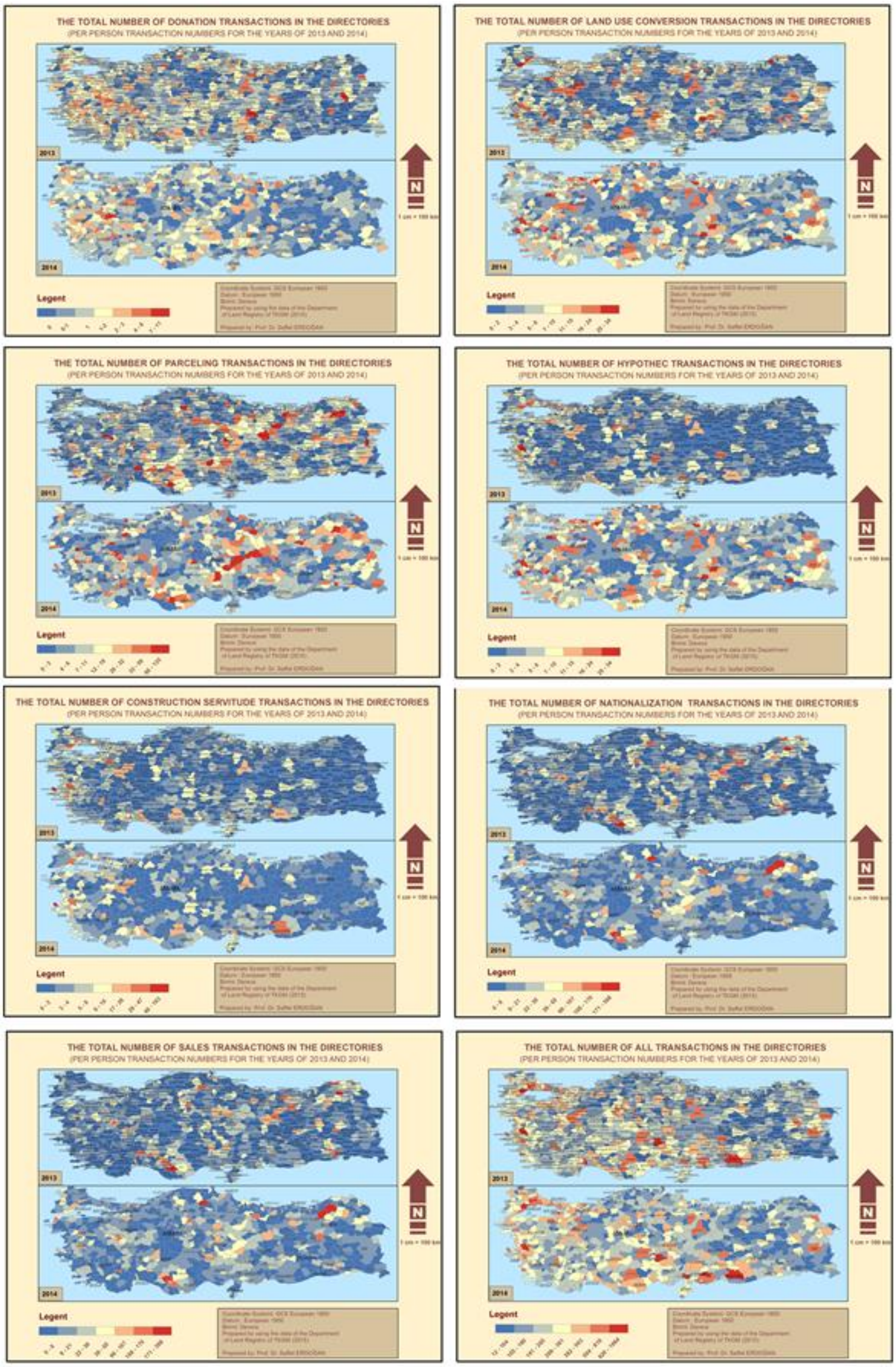

Figure 2: Per person transaction numbers in land registry directorates with EB smoothed values.

International Journal of Engineering and Geosciences (IJEG),
Vol; 4, Issue; 2, pp. 071-077, June, 2019,

If the excess risk value, which is obtained by rationing the actual number of cases by the estimated number of cases, equals one it means there is no difference between exposure and risk; if the value is above one there is an increased risk and if its below one there is a decreased risk. Hence, the structured excess risk maps are created by rationing the total number of actualized transactions performed in the land directorates by the ratio of estimated transaction numbers. Land directorates with values above one mean it is higher than the mean risk values with respect to the actualized transaction number; so they are problematic directorates in terms of transaction capacity (Figure 3).

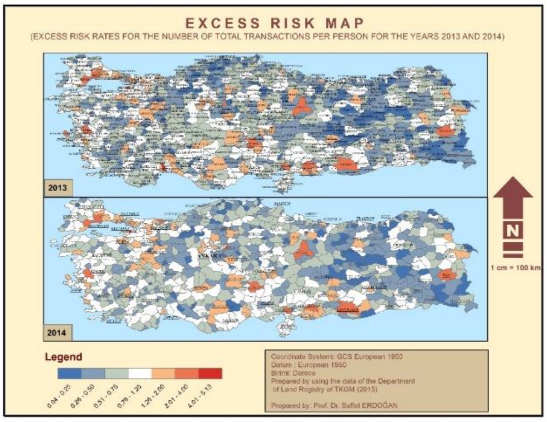

Figure 3: Excess risk map with respect to TSM transaction numbers.

Another spatial analysis performed using the ratios is spatial rate analysis, which is based on spatial moving areas. Instead of using independently estimated ratios for each TSM unit in a zone town, spatial rate analysis uses the mean value of ratios from other neighbors defined via neighborhood relations and determined with a weight matrix for each unit. In this analysis, depending on the number of identified neighbors, the values of units with high and low ratios are drawn closer to the neighborhood mean value by using neighbor values with the aim of determining regional and global changes. The critical issue here is the number of neighbors, as the number of neighbors is increased the raw ratio values become similar for the neighbor towns and once all neighbors are selected, the values of all towns become exactly the same (Anselin et al., 2006).

$$\pi = \frac{E_i + \sum_{j=1}^{j_i} E_j}{P_i + \sum_{j=1}^{j_i} P_j} \tag{3}$$

The results of spatial rate analysis conducted to visualize the regional and global changes in the number of actualized transactions in TSMs are shown in Figure 4.

In the next stage, based on the spatial dependency in a TSM zone defined by official territories, clustering sets were determined in terms of transaction numbers and per person transaction numbers and spatial auto-correlation, analyses were conducted.

In our study, after several tests, a weight matrix is formed by using the features of the seven closest neighborhoods, and Moran's I and Getis-Ord G* spatial auto-correlation methods were employed (Getis et al., 1992) (Moran, 1948).

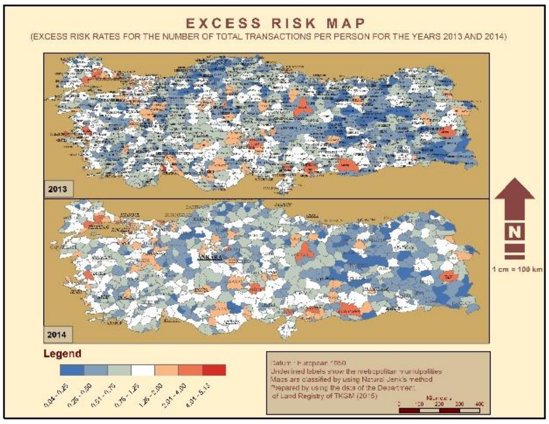

Figure 4: Regional changes and trends by spatial rate map with respect to the number of actualized transactions in TSMs.

The values that Moran's I spatial auto-correlation take vary between -1 and +1. Positive values indicate spatial clustering of the identical objects defined as hot or cold spots whilst negative values show the clustering of different objects defined as outlier points (4).

$$I_i = \frac{(X_i - \overline{X})}{S^2} \sum_j W_{ij} (X_j - X) \tag{4}$$

Although Moran's I index can produce the clustering of high and low values of objects, it fails to distinguish the objects from each other. This was expressed by Anselin (1995) who made some adaptations to Moran's I index and provided the LISA (local indicators of spatial association) index, which can produce a local-based clustering analysis. In LISA, statistically significant local clustering results are identified in four different categories as high-high, high-low, low-high, low-low. The TSM-related map produced by using LISA with respect to transaction numbers per person is shown in Figure 5.

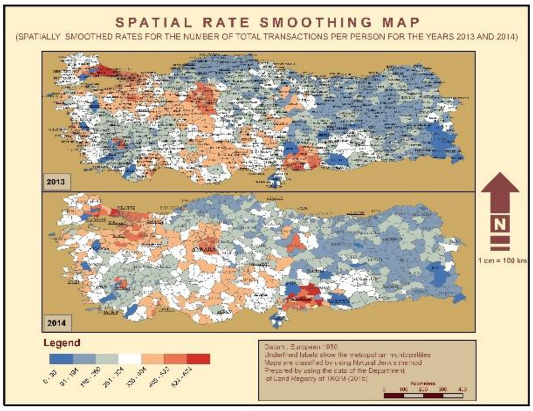

Figure 5: Transaction numbers per person using Moran's I clustering analysis.

International Journal of Engineering and Geosciences (IJEG),
Vol; 4, Issue; 2, pp. 071-077, June, 2019,

In the final stage of this analysis, a different spatial auto-correlation index, known as the Getis-Ord G* index, was used to compare the results. Unlike Moran's I index, Getis-Ord G* index is more sensitive in determining to cluster in high values. The positive values of Getis-Ord G* index take to mean the clustering of high-value objects, negative values mean the clustering of low-value objects and null value indicates randomness in the distribution of objects. The Getis-Ord G* index is generically used to compliment Moran's I index results and its formulation is as provided below. In Figure 6, the TSM-related map using clusters using based on the Getis-Ord G* index with respect to transaction numbers per person can be viewed.

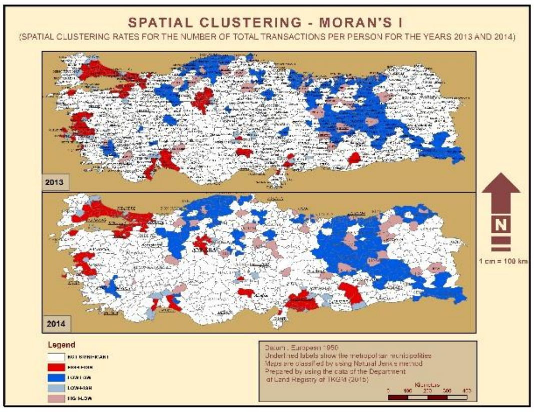

Figure 6: Transaction numbers per person using the Getis-Ord G clustering analysis

3. CONCLUSION AND DISCUSSION

In this study, GIS based spatial analyses have been exploited for human resource planning and employment relevant analysis in TSM. From the population figures and distribution per employee and as per a total number of employee volumes, there are approximately nine employees (standard deviation 10) in the directorates. The geographic distribution of directorates as per a number of total personnel shows that there is a homogeneous distribution. However, the standard deviation value of the number of personnel is higher since there exist many directorates whose values differ strongly from the mean values. Analysis of the geographic distribution of directorates with higher than average numbers of personnel shows that these directorates are mostly centered in metropolitan cities and central and western Anatolia. With respect to serviced population per person, it is detected that directorates located in the South East Anatolian Region and a few of the Metropolitan directorates are problematic (Figure 1). As the number of transactions per person is investigated it is seen that aside from the metropolitan directorates with high transaction volumes, there are density indicators in certain urban directorates (Kars, Nigde, Aksaray, Osmaniye, Tokat) (Figure 2). When the excess risk ratio of directorates with respect to work load is examined (Figure 3) it is seen that Yalova, Aksu, Cerkezköy, Bahcelievler, Corlu, Manisa, Osmaniye, Nigde, Gaziantep, Şanlıurfa, Sivas, Karaburun directorates have risk values six times above the mean risk value with respect to transaction numbers per person. When the results of spatial rate analysis conducted to understand regional and national changes in the number of transactions conducted per person in TSMs are examined it shows that directorates in İstanbul, Ankara, Gaziantep, Şanlıurfa cities are inclined towards an upper curve on a nationwide scale whilst the East of Turkey, including the complete territory of the Black Sea Region, is inclined towards a downward curve (Figure 4). In the present study, Moran's I and Getis-Ord G spatial analysis methods were employed to determine clustering sets of directorates that exhibit identical features. As the results of these analyses are examined, it is seen that both methods detected identical geographical regions.

Due to geographic, economic and cultural differences in Turkey's regions, a number of variations in the distribution of public services have been identified. GIS is a useful tool for making sound decisions by making the best usage of all available resources at global, national and regional scales with the aim of solving a wide range of problems, providing services, and managing both human and physical resources. The first stage for using GIS for public services is the visualization of statistics by means of appropriate mapping methods and thereby, enabling decision-making managers to make fast, accurate and effective decisions. In the second stage, a number of spatial statistical tests are conducted and according to the obtained results, directories exposing deficiencies can be determined with statistical significance.

The management and supervision of public services constitute a vital task for governments, public institutions, and organizations. By using GIS applications to analyse public services, it becomes easier to understand the distribution and condition of services in order to improve them and it is possible to make more effective decisions on where, when and what kind of resources to allocate. The present study is the first GIS based research in Turkey providing in-depth analysis of public human resource in Land Registry Directories within the scope of management and supervision of public services.

The application of GIS technology proves to be invaluable because it offers advanced analysis capabilities including the study of time series and overlay with additional spatial data layers like income, population composition and density, unemployment, literacy, etc. This can help to get insight into patterns of social and economic relationships that otherwise would have been left undetected.

REFERENCES

Sachs, J. D.; Mellinger, A. D., Gallup, J. L. (2001) The Geography of Poverty and Wealth. Scientific American. URL:http://www.joyhecht.net/East%20Africa%20Climate%20Change/Sachs%20geography%20of%20povery%20&%20wealth%20SciAm%202001.pdf

Tomlinson, R. F., Toorney, M.A.G. (1999). GIS and LIS in Canada. In: McGrath, G., Sebert, L. (eds.), Mapping a Northern Land: The Survey of Canada

1947-1994, McGill-Queen's University Press, Montreal, Quebec, Canada.

Tomlinson, R. F. (2011). Thinking About GIS: geographic information system planning for managers (4th ed.). ESRI Press. Redlands, CA.

Goodchild, M. (2004). Social Sciences: Interest in GIS Grows. ArcNews Online. Spring 2004. URL: http://www.esri.com/news/arcnews/spring04articles/social-sciences.html

Harries, K. (1999). Mapping Crime: Principle and Practice. Department of Justice. Washington, D.C.

Jan, A.K., Murty, M.N., Flynn, P.J. (1999). Data Clustering: A Review, ACM Computing Surveys, Vol. 31, No. 3, pp. 263-323.

P. Johnelle Sparks, Corey S. Sparks, Joseph J. A. Campbell (2013). An application of Bayesian spatial statistical methods to the study of racial and poverty segregation and infant mortality rates in the US. GeoJournal, 78:389–405.

Mitchell, A. (2005). The ESRI Guide to GIS Analysis. Volume 2: Spatial Measurements and Statistics. ESRI Press, Redlands, California.

Getis, A.; Ord, J. K. (1992). The Analysis Of Spatial Association By Use Of Distance Statistics. Geographical Analysis, 24, 11, pp. 189-206.

Oliver, D. R. (2005). Internal business functions. The GIS Guide for Local Government Officials. Redlands, CA.: ESRI Press, pp. 61-79.

İşcan, F., Ilgaz, A. (2017). Analysis Of Geographic/Urban Information System Web Presentations Of Local Goverments In Turkey, International Journal of Engineering and Geosciences, 2, 3, pp. 75-83.

Çabuk, S.N. (2015). GIS Use in Local Authorities and Urban Information Systems. Electronic Journal of Map Technologies. 7, 3, pp. 69-87.

Demirel, R., Erdoğan, S., Sözen, M. A. (2009). Determination Of High Risk Regions Of Human Brucellosis In Turkey Using Exploratory Spatial Analysis. Turkiye Klinikleri J Med Sci, 29, 1, pp. 25-35.

Erdoğan, S. (2009). Explorative Spatial Analysis Of Traffic Accident Statistics And Road Mortality Among The Provinces Of Turkey. Journal of Safety Research, 40, 5, pp. 341-355.

Fırat, M.; Dursun, Ö. F.; İnce, K.; Talu, M. F.; Aydoğdu, M. (2015). Coğrafi Bilgi Sistemlerin Kentsel Alt Yapı Sistemlerinde Kullanılması. ADYU Mühendislik Bilimleri Dergisi, 2, pp. 24-33.

Erdoğan, S.; Yalçın, M.; Dereli, M.A. (2013.) Exploratory spatial analysis of crimes against property in Turkey. Crime Law Social Change, 59, 1, pp. 63–78.

Ernst, F. (1996). Erstellung eines digitalen Umweltatlas für die Provinz Adana (Südtürkei) (A digital environmental atlas for the Province of Adana (southern Turkey)). Petermanns Geographische Mitteilungen. 140 (4): 217-226.

Türk, T. (2011). Türkiye'de Meydana Gelen Suçların Coğrafi Bilgi Sistemleri (CBS) ile İncelenmesi, hkm Jeodezi, Jeoinformasyon ve Arazi Yönetimi Dergisi, 1, 104, pp. 14-20.

Yuluğ, M. (1971). Kamu Kesiminde İstihdam Sorunu ve Yeni Personel Rejimi. Amme İdaresi Dergisi 4, 2, 46-51.

Dikmetaş, E.; İnan, N. (2000). Sağlık İnsan gücü Planlaması. 1. Ulusal Sağlık İdaresi Kongre Kitabı, Ankara, pp. 107-117.

Anselin, L., Lozano, L., Koschinsky, J. (2006). Rate Transformations And Smoothing. Spatial Analysis Laboratory Department Of Geography, University Of Illinois. Urbana-Champaign.

Moran, P. A. P. (1948). The interpretation of statistical maps. Journal of the Royal Statistical Society Series B-10, 36.

Anselin, L. (1995). Local ındicators Of Spatial Association-LISA. Geographical Analysis, 27, pp. 93-115.

International Journal of Engineering and Geosciences (IJEG),
Vol; 4, Issue; 2, pp. 078-087, June, 2019, ISSN 2548-0960, Turkey,
DOI: 10.26833/ijeg.455595

OBJECT BASED BURNED AREA MAPPING WITH RANDOM FOREST ALGORITHM

Resul Comert[1], Dilek Kucuk Matcı[2]*, Ugur Avdan [2]

[1] Gumushane University/Faculty of Engineering And Natural Sciences/Department Of Geomatic Engineering/ Gümüşhane, Turkey (rcomert@gumushane.edu.tr); **ORCID 0000-0002-0669-xxxx;**
[2] Institute of Space and Earth Sciences, Eskişehir Technical University, Eskişehir, Turkey, Turkey (dkmatci@anadolu.edu.tr, uavdan@eskisehir.edu.tr); **ORCID 0000-0002-8417-xxxx; ORCID 0000-0002-8417-xxxx;**

*Corresponding Author, Received: 28/08/2018, Accepted: 05/02/2019

ABSTRACT: It is very important to map the burned forest areas economically, quickly and with the high accuracy of issues such as damage assessment studies, fire risk analysis, and management of forest regeneration processes. Remote sensing methods give advantages such as fast, easy-to-use and high accuracy for burned area mapping. Recent years machine learning algorithms have become more popular in satellite image classification, due to the effective solutions for the analysis of complex datasets which have a large number of variables. In this study, the success of object based random forest algorithm was investigated for burned forest area mapping. For this purpose, Object based image analysis (OBIA) was performed using Landsat 8 image of the Adrasan and Kumluca fires which occurred in 24 – 27 June 2016. The study consisted of five steps. In the first step, the multi-resolution image segmentation was performed for obtaining image objects from Landsat 8 spectral bands. In the second step, the image object metrics such as spectral index and layer values were calculated for all image objects. In the third step, a random forest classifier model was developed. Then, the developed model applied to the test site for classification of the burned area. Finally, the obtained results evaluated with confusion matrix based on the randomly sampled points. According to the results, we obtained 0.089 commission error (CE) with 0.014 omission error (OE). An overall accuracy was obtained as 0.99. The results show that this approach is very useful to be used to determine burned forest areas.

Keywords: *Random forest, Burned area mapping, Object based image analysis, Remote sensing*

1. INTRODUCTION

Forests, one of the most important natural sources, provide a rich biodiversity that contributes directly and indirectly to economic and social life. The destruction of forests by fire leads to negative effects such as environmental pollution, destruction of historical and natural wealth, picnic places, forest parks, hunting areas and sports areas that are suitable for the city life and adversely affecting the economy (Adams, 2013).

Especially for the countries located in the Mediterranean climate zone, forest fires are among the most important natural threats (Hernandez, Drobinski, & Turquety, 2015). About 50,000 fires occur each year in these countries and about 700,000-1,000,000 ha of forest area are exposed to fire (Dimitriou, Mantakas, & Kouvelis, 2001). Mapping burned areas can determine the effects of fires (G. Chen et al., 2017; Meng et al., 2017; Palandjian, Gitas, & Wright, 2009) and help to plan and manage operations to prevent desertification, biodiversity loss, flooding and soil erosion, which can occur after a fire (Vallejo, Arianoutsou, & Moreira, 2012). It can also be used as input data for the generation of fire risk maps of the future(Filippidis & Mitsopoulos, 2004).

Satellite remote sensing has offered great advantages in the monitoring and mapping of burned areas since the 1980s (Flannigan & Haar, 1986). Optical satellite data has been especially successful in generating a burned area inventory on the continental scale (Barbosa, Grégoire, & Pereira, 1999), regional scale (Giglio, Loboda, Roy, Quayle, & Justice, 2009; Loboda, O'neal, & Csiszar, 2007) and national scale(Palandjian et al., 2009). Many image analysis techniques, such as vegetation and burn index (Chuvieco, Martin, & Palacios, 2002; Epting, Verbyla, & Sorbel, 2005; Escuin, Navarro, & Fernandez, 2008; Loboda et al., 2007; Pereira, 1999), supervised classification (Palandjian et al., 2009), logistic regression (Bastarrika, Chuvieco, & Martín, 2011), spectral angle mapper and artificial neural network (Petropoulos, Vadrevu, Xanthopoulos, Karantounias, & Scholze, 2010), Neuro-fuzzy (Mitrakis, Mallinis, Koutsias, & Theocharis, 2012) and support vector machine (Petropoulos, Kontoes, & Keramitsoglou, 2011), have been successfully applied to pixel based satellite data of various resolutions.

Pixel based image analysis (PBIA) and object based image analysis (OBIA) techniques are the two main image analysis approach in satellite image classification. While PBIA approach works on each individual pixel for extracting information from satellite images, OBIA approach uses image objects that consist of homogenous pixel groups. While pixel based approach has generally applied to medium and low spatial resolution images, OBIA has applied to high and very high spatial resolution images. There were many studies that applied to OBIA to medium and low resolution images for burned area mapping (Gitas, Mitri et al. 2004, Polychronaki and Gitas 2012, Katagis, Gitas et al. 2014, Kavzoglu, Erdemir et al. 2016), (Gitas, Mitri et al. 2004). Analyzing the studies using medium resolution satellite images to compare these two approaches, OBIA gives more accurate results than PBIA (Estoque, Murayama, & Akiyama, 2015; Gao, Mas, Kerle, & Pacheco, 2011; Gilbertson, Kemp, & van Niekerk, 2017; Varamesh, Hosseini, & Rahimzadegan, 2017). Also, OBIA reduce the salt and pepper effect that cause misclassified pixel on satellite images (Phiri & Morgenroth, 2017)(Gao et al. 2011). For these reasons, OBIA was selected for burned forest area mapping in this study.

Object-based classification of burned areas has been applied to very high-resolution images (Dragozi, Gitas, Stavrakoudis, & Theocharis, 2014), high-resolution images (Sertel & Alganci, 2016), medium resolution images (Katagis, Gitas, & Mitri, 2014; Kavzoglu, Erdemir, & Tonbul, 2016; Mitri & Gitas, 2004; Polychronaki & Gitas, 2012), low resolution images (Gitas, Mitri, & Ventura, 2004) and SAR images(Polychronaki, Gitas, Veraverbeke, & Debien, 2013). The OBIA has two main steps, segmentation and classification (Baatz, Hoffmann, & Willhauck, 2008). Multi-resolution segmentation used in the segmentation phase is a preferred method (Benz, Hofmann, Willhauck, Lingenfelder, & Heynen, 2004). The classification process is carried out by rule-based or supervised classification.

In many studies, rule-based classification methods have been used to map burned areas along with object-based classification methods. The rule-based classification has two limitations, although it does not yield successful results in the removal of burned areas. These are, (i) the difficulty in deciding which descriptive properties are really important within a large number of object metrics in large data sets, and (ii) its limited applicability to different environmental conditions and different data types (Stumpf & Kerle, 2011). Therefore, in the extraction of burned fields from complex datasets and data sets with a large number of variables, there is a need to implement other classification algorithms. Machine learning algorithms such as random forest (Breiman, 2001) provide effective solutions for the analysis of complex datasets. Random forest has been successfully applied to areas such as mapping landslides (Breiman, 2001; W. Chen, Li, Wang, Chen, & Liu, 2014; Stumpf & Kerle, 2011), gene selection (Díaz-Uriarte & De Andres, 2006), land cover classification (Gislason, Benediktsson, & Sveinsson, 2006) and hyperspectral image classification (Ham, Chen, Crawford, & Ghosh, 2005). Also, it has been used forest fire studies such as fire occurrence modeling (Gislason et al., 2006), forest and woodland severity analysis (Dillon et al., 2011; Holden, Morgan, & Evans, 2009). There is only one study is available in the literature for the mapping of burned areas with the random forest based classifier. This classifier was developed to extract the burned areas on the global scale from the MODIS images (Ramo & Chuvieco, 2017).

In this study, we evaluated the performance of the random forests algorithm for mapping of burned forest areas from remotely sensed images that were segmented to image objects. This approach allows the advantages of an object-based classification method to combine random forest algorithm with more accurate extraction of burned areas.The images of the Kumluca and Adrasan regions (the study area) are obtained for free from the Landsat 8 satellite. First, the images are segmented using multi-resolution segmentation for obtaining image objects. After the image object attributes such as band indices and band value were calculated, training and test datasets were generated. The training data were used to determine the optimal random forest classification model by testing different parameter and attribute importance for best result is calculated. The classification model was applied to test data set. The accuracy level of the results was

International Journal of Engineering and Geosciences (IJEG),
Vol; 4, Issue; 2, pp. 078-087, June, 2019, ,

evaluated according to the confusion matrix based on the randomly sampled points. Also, the map obtained from the local authority and the map obtained by the proposed method were compared according to the total burned areas. In addition, Normalize Difference Vegetation Index (NDVI) based change detection map was used for interpretation of results. The results show that the random forest algorithm has the potential to be used as a tool by forest management authorities to identify burned forest areas with high accuracy and low cost.

2. STUDY AREA AND DATA SETS

In this study, the forest fires that occurred on 24-27 June 2016 in Adrasan and Kumluca regions in Antalya province were investigated (Figure 1). The province of Antalya is located in the Mediterranean climate zone, where there is a risk of first-degree fire. The existing forest area is 1,146,062 hectares, covering 56% of the province's surface area. The forest areas in the province correspond to 5.4% of the forest areas of Turkey. The tree species in the Antalya forest area are composed of the red leaf (65%), cedar (16%), black cherry (8%), fir (5%), juniper (4%) and other leafy species (URL 1). During the fire that occurred on 24 – 27 June 2016, very large forest areas were destroyed, animals, greenhouses and houses were badly affected (Neyisci, Sirin, Bas, & Saribasak, 2016).

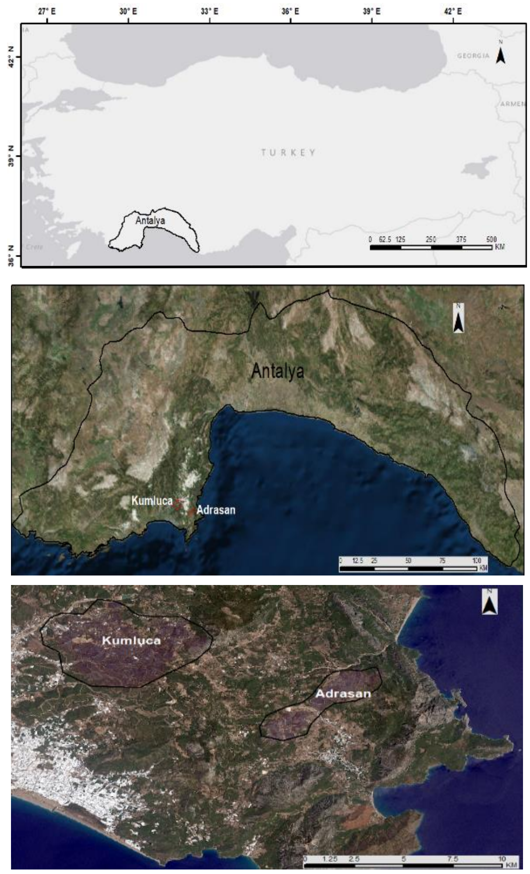

Figure. 1 Location of Adrasan and Kumluca

Landsat 8 Operational Land Imager (OLI) L1TP post-event (08 July 2016) data were used in this study. The Landsat L1TP collection is radiometrically calibrated and orthorectified using ground control points and digital elevation model (DEM) data, to correct for relief displacement (URL 2). Post-event image bands were used for mapping the area with random forest. Landsat 8 OLI sensor images consist of nine spectral bands. Excluding the cirrus and ultra-blue bands, seven bands were used for burned area analysis (Table 1). Also, pre-event image (which was taken 22 June 2016) was utilized for obtaining NDVI based change detection map.

Table 1 Landsat 8 OLI bands, wavelengths and image resolutions

Band	Wavelength (micrometers)	Resolution (meters)
Band 2	0.452 – 0.512	30
Band 3	0.533 – 0.590	30
Band 4	0.636 – 0.673	30
Band 5	0.851 – 0.879	30
Band 6	1.566 – 1.651	30
Band 7	2.107 – 2.294	30
Band 8	0.503 – 0.676	15

3. METHODS

In this study, applied methods was composed of five steps which were pre-processing, image segmentation, calculation of image object attributes, classification and accuracy assessment.

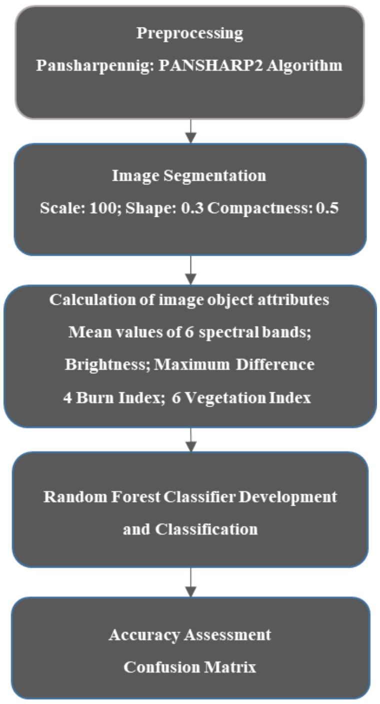

Figure. 2 Flowchart of the methodology for burned area classification

3.1 Preprocessing

During the preprocessing phase, 30-meter spectral bands were pansharpened with a panchromatic band of the 15 - meter resolution. In this phase, the PANSHARP2 algorithm in PCI Geomatica (2016) software was used for fusion of panchromatic and spectral bands. This versatile and extremely simple algorithm that can work with any data type is based on the least squares and a statistical approach. The first step in the PANSHARP 2 algorithm is to co-register the panchromatic band and multi-spectrum image bands together as geographically corrected. This algorithm attempts to protect spectral properties, mean, standard deviation, and histogram shape for each channel. When calculating the best gray value with the smallest squares and color presentation, statistical approximation and automatic fusion were performed (Zhang, 2002).

3.2 Image Segmentation

In this study, the advantages of the object-based classification method were used to obtain a more accurate result. This method has been used in the literature to overcome the limitations and weaknesses of pixel based image analysis.

The first stage of object-based classification is the creation of homogeneous and meaningful image objects for image segmentation. Over recent decades, a number of image segmentation methods have been developed for remote sensing image analysis (Dey, Zhang, & Zhong, 2010). In this study, the multi-resolution segmentation (MRS) method was used. MRS is a region enhancement algorithm that combines pixels or existing image objects together. The method starts at the pixel level and combines neighboring pixels depending on a spectral and geometric homogeneity criterion. In the study, MRS was implemented using Ecognition Developer (version: 9.0) software. In the segmentation process, 6 spectral bands, which are pansharpened to 15m, were used. In order to obtain optimal image objects, the scale parameter, shape, integrity and layer weight were specified by the user (Benz, Hofmann, Willhauck, Lingenfelder, & Heynen, 2004). As a result of a visual analysis made by the trial and error method, the appropriate parameter values for the data set were determined as scale factor 100, shape 0.3 and compactness 0.5. The equal weight values were assigned to all bands.

3.3 Calculation of Image Object Attributes

The forest fires directly affect the vegetation. There are many studies on burned area mapping and burned severity assessment use burned area indices and vegetation indices for increasing success of the methods (Chuvieco et al., 2002; Fraser, Li, & Cihlar, 2000; Loboda et al., 2007; Schepers et al., 2014). Starting from that, commonly used indices and other band values were preferred object image attributes. Eighteen object attributes were calculated for use in the classification steps of random forest, described below:

The mean values of six spectral bands (Blue, Green, Red, NIR, SWIR 1, SWIR 2), defined as the average of the reflection values of the pixels that form an image object.

The mean brightness (B) calculated as the sum of the object means in the bands $(\overline{c}_{i(vis)})$ divided by the number of the corresponding bands (n_{vis}) (Stumpf & Kerle, 2011):

$$B = (1/n_{vis}) \sum_{i=1}^{n_{vis}} \overline{c}_{i(vis)} \tag{1}$$

The maximum difference, defined as the absolute value of the difference between the minimum object mean $\min(\overline{C}_{i(vis)})$ and maximum object mean $\max(\overline{C}_{i(vis)})$, divided by the object brightness B (Stumpf & Kerle, 2011):

$$MaxDiff = (max(\overline{c}_{i(vis)}) - min(\overline{c}_{i(vis)})) / B \tag{2}$$

Four burned area indexes, as frequently referred to in the literature, calculated for image objects: burned area index (BAI), normalized burn ratio (NBR) (Key & Benson, 2006), normalized burn ratio 2 (NBR2), and mid-infrared burn index (MIRBI) (Trigg & Flasse, 2001):

$$BAI = 1/((0.1 - Red)^2 + (0.06 - NIR)^2) \tag{3}$$

$$NBR = (NIR - SWIR2)/(NIR + SWIR2) \tag{4}$$

$$\mathrm{NBR2} = (\mathrm{SWIR1} - \mathrm{SWIR2})/(\mathrm{SWIR1} + \mathrm{SWIR2}) \tag{5}$$

$$MIRBI = 10\,SWIR2 - 9.8\,SWIR1 + 2 \tag{6}$$

Six spectral indices for burned area and fire damage detection, the normalized difference vegetation index (NDVI) (Tucker, 1979), global environmental monitoring index (GEMI) (Pinty & Verstraete, 1992), enhanced vegetation index (EVI)(A. Huete et al., 2002), soil-adjusted vegetation index (SAVI) (A. R. Huete, 1988), char Soil Index (CSI) (Smith et al., 2007) and normalized difference moisture index (NDMI) (Wilson & Sader, 2002). The equation for:

$$\mathbf{NDVI = (NIR - RED)/(NIR + RED)} \tag{7}$$

$$\mathrm{GEMI} = \gamma(1 - 0.25\gamma) - (\mathrm{RED} - 0.125)/(1 - \mathrm{RED}) \tag{8}$$

with

$$\gamma = ((2\mathrm{NIR})^2 - \mathrm{RED}^2 + 1.5\mathrm{NIR} + 0.5\mathrm{R})/(\mathrm{NIR} + \mathrm{RED} + 0.5) \tag{9}$$

$$\mathbf{EVI = 2.5 * ((NIR - RED)/(NIR - 6RED - 7.5BLUE + 1))} \tag{10}$$

$$\mathrm{SAVI} = (1 + \mathrm{L})((\mathrm{NIR} - \mathrm{RED})/(\mathrm{NIR} + \mathrm{RED} + \mathrm{L})) \tag{11}$$

with

$$L = 0.5 \quad (12)$$

$$CSI = NIR/SWIR2 \quad (13)$$

$$NDMI = (NIR - SWIR1)/(NIR + SWIR1) \quad (14)$$

3.4 Classification

The random forest method, which is a machine learning algorithm, is used for the classification of the burned areas. The random forest method, developed by Breiman (2001), is a nonparametric mass learning algorithm that uses numerous decision trees in the classification process (Breiman, 2001). According to Breiman (Breiman, 1996), with a classification process using a single decision tree, small changes in training lead to high variance. And this situation reduces the accuracy of classification. Random forest, on the other hand, forms a multi-decision tree with sub-datasets randomly selected in the training data. Each decision tree is voted for, according to its class membership, and the decision tree that receives the most votes is used in predicting the related class (Stumpf & Kerle, 2011).

The random forest algorithm works according to the supervised classification method. In this context, training and test data are needed. Within the scope of the study, the Kumluca region was selected as the training area and the Adrasan region as the test area. In the training area, image segments were defined in two classes, burned area (BA) and non-burned area (NBA). There are 13551 number of the image objects in the training data field. The 501 number of them were burned areas, and the others were non-burned areas. There are 9968 image segments in the test data (Figure 3).

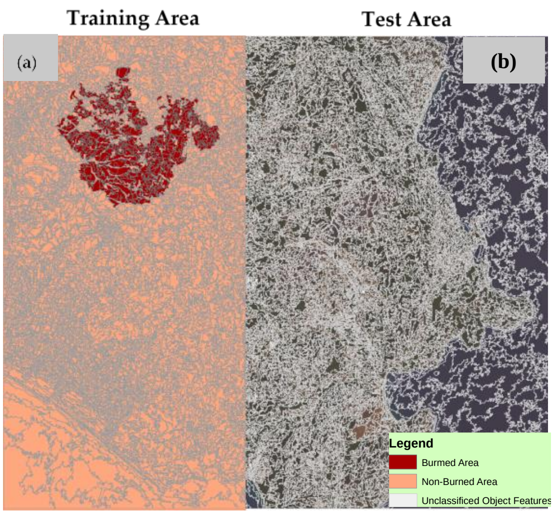

Figure 3. (a) Kumluca training area included 501 burned areas (BA) image objects and 13050 non-burned area image objects; (b) Adrasan test site included 9968 unclassified image objects

In the study, the model parameters to be used in the classification of the training data were determined first. In the random forest algorithm, there are two parameters must be determined by the user. These are the number of trees (N) and the number of attributes to choose randomly (m). These two parameters were applied to the training data with various values, in order to find the appropriate model values for classification. The m value was generally calculated using √m equation. 20 different random forest classifier models which were a combination of the ten numbers of trees (100-1000 increase by 100) and two numbers of attributes (m = 4, 5 which indicate integer value the lower and upper values close to √m) was built for determining the optimum parameter. The result was evaluated Balanced Accuracy (Kuhn & Johnson, 2013; Ramo & Chuvieco, 2017) defined in Table 2.

$$\text{Balanced Accuracy} = \left(\frac{E11}{(E11+E21)} + \frac{E22}{(E22+E12)}\right)/2 \quad (15)$$

Table 2. Structure of Burned Area Confusion Matrix

	Reference		
Predicted	Burned	Non – Burned	Row Total
Burned	E_{11}	E_{12}	E_{1+}
Non – Burned	E_{21}	E_{22}	E_{2+}
Col. Total	E_{+1}	E_{+2}	$E_{\sum}$

3.5 Accuracy Assessment

The random forest classification results were validated using a confusion matrix, known as the most common method of image classification in remote sensing applications. It was possible to calculate overall accuracy, omission errors and commission errors using the confusion matrix (Banko, 1998). Classification results which applied to test data evaluated two different ways. First, 650 random points were generated for evaluation of the classification results. Then the result was compared local authority map. Following equation shows error value calculations. A parameter which is used in equation same as the Table 2.

$$\text{Omission Error} = (E_{+1} - E_{11})/E_{+1} \quad (16)$$

$$\text{Commission error} = (E_{1+} - E_{11})/E_{1+} \quad (17)$$

$$\text{Overall Accuracy} = (E_{11} - E_{22})/E_{\sum} \quad (18)$$

4. RESULTS

4.1 Optimum parameter selection for Random Forest (RF)

Developing of random forest classifier, open source WEKA Data Mining software was used for burned forest area mapping. random forest algorithm was applied to the training data as ten-fold cross-validation procedure. In this purpose, the data were randomly divided into ten parts. Nine parts are used as training data and one part is used as validation data. This step continues in a way that all parts are applied alternately. The 20 different classifier model was developed according to two attribute' s value

International Journal of Engineering and Geosciences (IJEG),
Vol; 4, Issue; 2, pp. 078-087, June, 2019, ,

(4,5) and ten different numbers of trees (100-1000 increase by 100). Figure 4 shows the balanced accuracy of 20 models according to the different number of randomly selected attributes (m) and the number of trees (N). It was also tested in other values that are different from the attribute numbers 4 and 5. The similar results were obtained for other numbers of attributes. Therefore, only 4 and 5 attributes value result is shown in Figure 4. According to Figure optimum parameters were selected as N = 400 and m = 5 which give higher balanced accuracy (0.914).

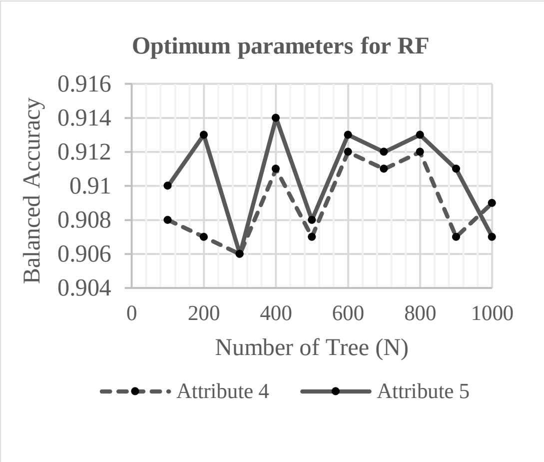

Figure 4. Balanced Accuracy value for different number of randomly selected attributes and number of trees.

4.2 Attributes Importance

The spectral bands in remote sensed images and spectral indices obtained with the help of these bands provide a wide range of variable. The use of these detailed variable increases the processing time as much information does not always provide the right result. Therefore, it should be determined which features are important for classification to reduce the data size.

The attribute importance was calculated with the different methods in the literature (Biau, Devroye, & Lugosi, 2008; Ishwaran, 2007; Louppe, Wehenkel, Sutera, & Geurts, 2013; Meinshausen, 2006). In their study, Louppe at.all (2013) indicate that the average impurity decrease value for each input variable is equal to zero only if the variable is irrelevant.

In this study attribute importance was calculated according to the average impurity decrease for selected optimum random forest parameters (Louppe et al., 2013). Figure 5 shows the importance of every attribute which was used in this study. All attributes have very closed importance each other. But NDVI has seen the most important attributes which have 0.34 impurity decrease. GEMI and EVI indices that have 0.32 impurity decrease are secondly important attributes. According to attributes importance results there is no variable that equal to zero. Therefore, all attributes were used for classification.

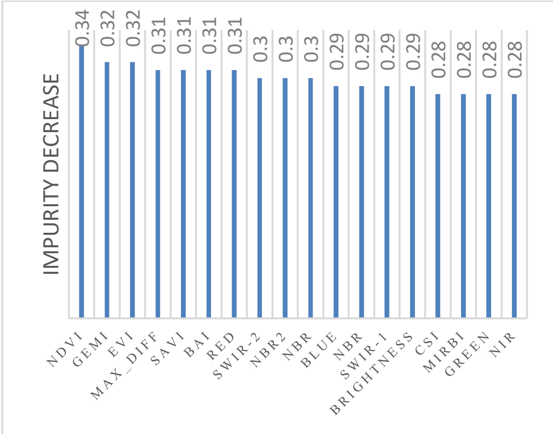

Figure 5. Attribute importance based on the average impurity decrease.

4.3 Random Forest Classification Results for Adrasan Test Site

The developed random forest classifier model for training data based on optimum parameters was applied the test dataset. The obtained results were evaluated with two different ways. First, randomly 650 points were generated on a test site to evaluate the classification results. Then, obtained map compare with local authority map.

According to the random points results, the object based random forest classification achieves 0.089 commission error (CE) with 0.014 omission error (OE). An overall accuracy was obtained as 0.99. Table 3 shows the error matrix with descriptive statistics.

Table 3. Accuracy assessment using 650 random points for object-based random forest classification, overall accuracy (OA), omission error (OE) and commission error (CE) estimated based on confusion matrix. (BA: Burned Area; NBA: Non-Burned Area)

	Reference				
Classification	BA	NBA	TOTAL	CE	OE
BA	71	7	78	0.089	0.014
NBA	1	571	572	0.017	0.012
Total	72	578	650		
		Overall Accuracy		0.987	

The random forest classification result compared with a local authority map which was generated by the Antalya Forest General Directorate. Table 4 shows evaluation results. According to the Table 4, the total area of the burned forest is in the map obtained from local authority 609.48 ha, in the result map of the classification 483.98 ha. The difference between them is 125.5 ha.

Table 4. Comparison of the result of random forest classification and the map obtained from local authority (unit: hectares)

Local Map	Random Forest Classification	Difference
609.48	483.98	125.5

5. DISCUSSION

In the segmentation process, the similar pixels were grouped based on the object-based classification method. This process reduced the number of input data for classification process. in the analysis to ensure quick results. In the study, after the segmentation process the number of the input data to be classified decreased from 1762725 to 23519.

The random forest algorithm is a fast-running classification method that can be applied to a large number of data and variables. In the study, burned areas were successfully determined using the 18 variables. Since the variables were randomly selected in the classification process with the random forest algorithm, in each classification, different variables could be included. Also, which attributes are important for classification could be calculated.

In this study, a random forest classifier model was developed for Landsat 8 data. The developed model was tested on Adrasan burned area. Evaluation of results two different reference data which area 650 random points and the local authority map was used. Ground truth for 650 random points was labeled using the RGB color map of Landsat 8, Google Earth images and NDVI difference maps. 650 random points results give higher accuracy with 0.089 commission and 0.014 omission error.

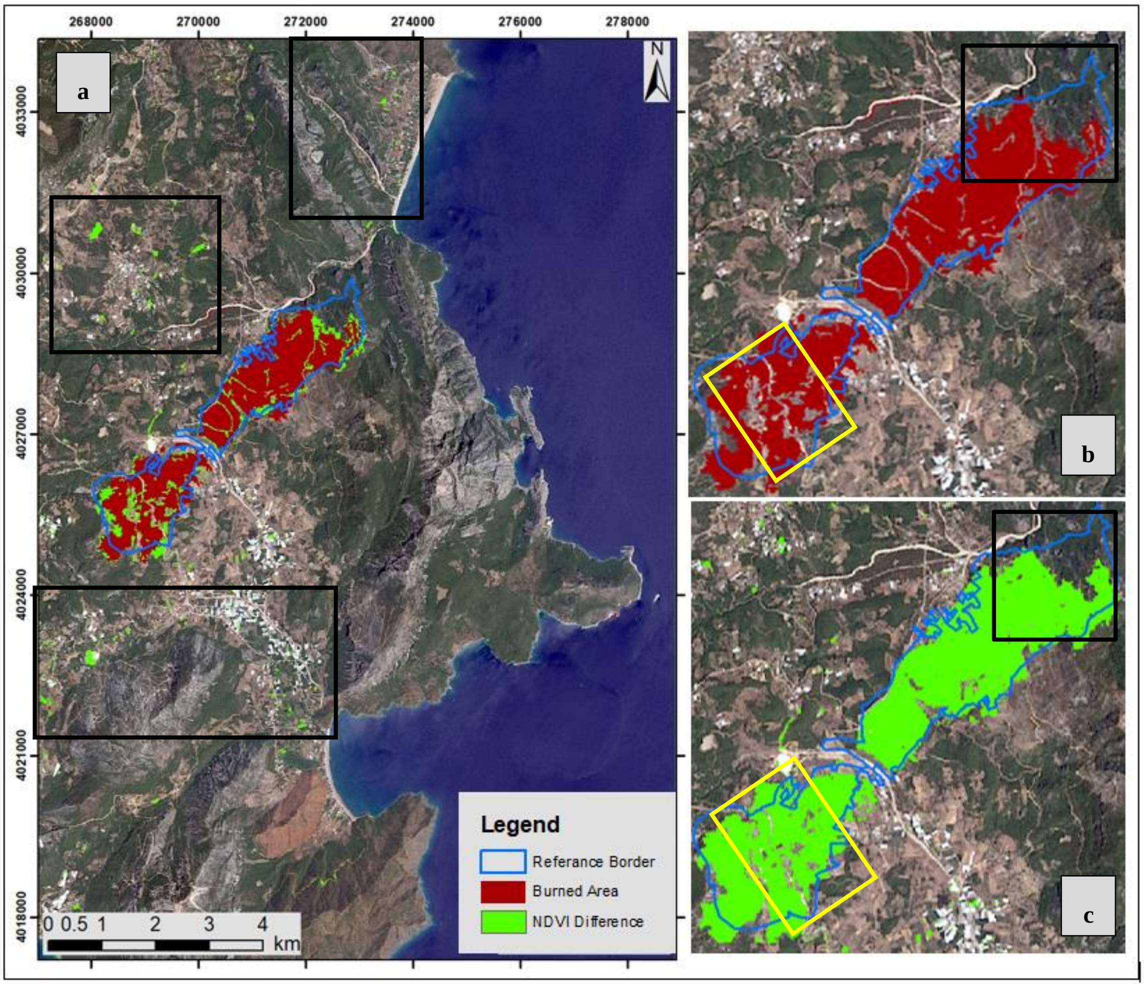

Figure 6. (a): Overlapped of the local map, NDVI difference map and random forest classification results for burning areas, the black rectangle indicates areas with NDVI change similar to burned areas. (b): local burned area border and random forest classification results, the black rectangle shows unchanged vegetation area, the yellow rectangle indicates soil and road area. (c): local burned area border and NDVI difference results, black rectangle shows unchanged vegetation area, the yellow rectangle indicates soil and road area.

The NDVI difference map was generated for interpretation of the results. Pre-event (22 June 2016) NDVI map was extracted from the post-event (8 July 2016) NDVI map for generating NDVI difference map (dNDVI). Figure 6 shows the local authority burned area border as a blue line, dNDVI results as green color and random forest classification results as red color. According to Figure 6a, the results of dNDVI and random forest classification results largely overlapped, while the local authority map shows a wider area than both. Although there is no change in plant cover in the areas indicated by black rectangles in figures 6b and 6c, these areas are shown as a burned area in the local map. Local authority burned area boundary shows a more general area. While the local map showed a general area, the results of the dNDVI map and the random forest classification did not reveal the soil and road areas as burned areas which shows a yellow rectangle in figure 6b and figure 6c. These results explain where the difference area in Table 4 came from.

Forest fires are disasters that directly affect the forest cover. If the burning area is below the forest and there is no change in the forest, mapping it from optical satellite images is not possible. In figure 6b, the area shown by the black rectangle was not mapped with applied method in this study, because forest cover has not changed. On the other hand, change detection analysis made by one attribute such as NDVI, other surfaces could be extracted as burned area. For example, Areas which are shown by the black rectangle in figure 6a has similar NDVI change with the burned areas. In addition, pre-event and post-event images are not always easy to access. Therefore, classification algorithms such as random forests, which can use many attributes over a single image, are very important. In this study, the random forest algorithm was applied at the local scale, but this study can be applied to larger areas.

6. CONCLUSION

The rapid development of remote sensing technologies has prompted users to look for ways to develop powerful and effective alternatives at the point of delivery analysis. In recent years, fast and efficient classification algorithms have been developed for classifying data in complex structures, particularly in the classification of satellite images for the production of thematic maps. Among these methods, machine learning algorithm called random forest algorithm is proposed as an effective classification algorithm which is used to solve many application problems including the problem of classification of remotely sensed images.

In this study, a random forest algorithm searched for potential burned areas. 18 variables were used (10 spectral indexes, mean values of 6 bands, brightness, and maximum difference), taken from the literature, to identify burned areas. Since the random forest algorithm randomly selects variables in the classification process, it can be seen that each experiment could benefit from using different variables. As a result of the classification process, the burned areas were determined with a high level of accuracy. The study was carried out in two burned forest areas, on the same date. The Kumluca area was used as training data and the Adrasan area as test data. The results of the classification process show that this method could be used for identifying burned areas with the high accuracy. Future studies will be based on to use the method on the higher resolution images such as Sentinel -2 which provide free data to improve the field of use.

REFERENCES

Adams, M. A. (2013). Mega-fires, tipping points and ecosystem services: Managing forests and woodlands in an uncertain future. Forest Ecology and Management, 294, 250-261.

Banko, G. (1998). A review of assessing the accuracy of classifications of remotely sensed data and of methods including remote sensing data in forest inventory.

Barbosa, P. M., Grégoire, J.-M., & Pereira, J. M. C. (1999). An algorithm for extracting burned areas from time series of AVHRR GAC data applied at a continental scale. Remote Sensing of Environment, 69(3), 253-263.

Bastarrika, A., Chuvieco, E., & Martín, M. P. (2011). Mapping burned areas from Landsat TM/ETM+ data with a two-phase algorithm: Balancing omission and commission errors. Remote Sensing of Environment, 115(4), 1003-1012.

Benz, U. C., Hofmann, P., Willhauck, G., Lingenfelder, I., & Heynen, M. (2004). Multi-resolution, object-oriented fuzzy analysis of remote sensing data for GIS-ready information. ISPRS Journal of photogrammetry and remote sensing, 58(3), 239-258.

Biau, G., Devroye, L., & Lugosi, G. (2008). Consistency of random forests and other averaging classifiers. Journal of Machine Learning Research, 9(Sep), 2015-2033.
Breiman, L. (1996). Bagging predictors. Machine learning, 24(2), 123-140.

Breiman, L. (2001). Random forests. Machine learning, 45(1), 5-32.

Chen, G., He, Y., De Santis, A., Li, G., Cobb, R., & Meentemeyer, R. K. (2017). Assessing the impact of emerging forest disease on wildfire using Landsat and KOMPSAT-2 data. Remote Sensing of Environment, 195, 218-229.

Chen, W., Li, X., Wang, Y., Chen, G., & Liu, S. (2014). Forested landslide detection using LiDAR data and the random forest algorithm: A case study of the Three Gorges, China. Remote Sensing of Environment, 152, 291-301.

Chuvieco, E., Martin, M. P., & Palacios, A. (2002). Assessment of different spectral indices in the red-near-infrared spectral domain for burned land discrimination. International Journal of Remote Sensing, 23(23), 5103-5110.

Dey, V., Zhang, Y., & Zhong, M. (2010). A review on image segmentation techniques with remote sensing perspective: na.

Díaz-Uriarte, R., & De Andres, S. A. (2006). Gene selection and classification of microarray data using random forest. BMC bioinformatics, 7(1), 3.

Dillon, G. K., Holden, Z. A., Morgan, P., Crimmins, M. A., Heyerdahl, E. K., & Luce, C. H. (2011). Both topography and climate affected forest and woodland burn severity in two regions of the western US, 1984 to 2006. Ecosphere, 2(12), 1-33.

Dimitriou, A., Mantakas, G., & Kouvelis, S. (2001). An analysis of key issues that underlie forest fires and shape subsequent fire management strategies in 12 countries in the Mediterranean basin. Final report prepared by Alcyon for WWF Mediterranean Programme Office and IUCN.

Epting, J., Verbyla, D., & Sorbel, B. (2005). Evaluation of remotely sensed indices for assessing burn severity in interior Alaska using Landsat TM and ETM+. Remote Sensing of Environment, 96(3), 328-339.

Escuin, S., Navarro, R., & Fernandez, P. (2008). Fire severity assessment by using NBR (Normalized Burn Ratio) and NDVI (Normalized Difference Vegetation Index) derived from LANDSAT TM/ETM images. International Journal of Remote Sensing, 29(4), 1053-1073.

Estoque, R. C., Murayama, Y., & Akiyama, C. M. (2015). Pixel-based and object-based classifications using high- and medium-spatial-resolution imageries in the urban and suburban landscapes. Geocarto International, 30(10), 1113-1129.

Filippidis, E., & Mitsopoulos, I. (2004). Mapping forest fire risk zones based on historical fire data in Mount Olympus, Greece, using geographical information systems. WIT Transactions on Ecology and the Environment, 77.

Flannigan, M. D., & Haar, T. V. (1986). Forest fire monitoring using NOAA satellite AVHRR. Canadian Journal of Forest Research, 16(5), 975-982.

Fraser, R., Li, Z., & Cihlar, J. (2000). Hotspot and NDVI differencing synergy (HANDS): A new technique for burned area mapping over boreal forest. Remote Sensing of Environment, 74(3), 362-376.

Gao, Y., Mas, J. F., Kerle, N., & Pacheco, J. A. N. (2011). Optimal region growing segmentation and its effect on classification accuracy. International Journal of Remote Sensing, 32(13), 3747-3763.

Giglio, L., Loboda, T., Roy, D. P., Quayle, B., & Justice, C. O. (2009). An active-fire based burned area mapping algorithm for the MODIS sensor. Remote Sensing of Environment, 113(2), 408-420.

Gilbertson, J. K., Kemp, J., & van Niekerk, A. (2017). Effect of pan-sharpening multi-temporal Landsat 8 imagery for crop type differentiation using different classification techniques. Computers and Electronics in Agriculture, 134, 151-159.

Gislason, P. O., Benediktsson, J. A., & Sveinsson, J. R. (2006). Random forests for land cover classification. Pattern Recognition Letters, 27(4), 294-300.

Ham, J., Chen, Y., Crawford, M. M., & Ghosh, J. (2005). Investigation of the random forest framework for classification of hyperspectral data. IEEE Transactions on Geoscience and Remote Sensing, 43(3), 492-501.

Hernandez, C., Drobinski, P., & Turquety, S. (2015). How much does weather control fire size and intensity in the Mediterranean region? Annales Geophysicae, 33(7), 931-939.

Holden, Z. A., Morgan, P., & Evans, J. S. (2009). A predictive model of burn severity based on 20-year satellite-inferred burn severity data in a large southwestern US wilderness area. Forest Ecology and Management, 258(11), 2399-2406.

Huete, A., Didan, K., Miura, T., Rodriguez, E. P., Gao, X., & Ferreira, L. G. (2002). Overview of the radiometric and biophysical performance of the MODIS vegetation indices. Remote Sensing of Environment, 83(1), 195-213.

Huete, A. R. (1988). A soil-adjusted vegetation index (SAVI). Remote Sensing of Environment, 25(3), 295-309.

Ishwaran, H. (2007). Variable importance in binary regression trees and forests. Electronic Journal of Statistics, 1, 519-537.

Key, C., & Benson, N. (2006). Landscape assessment: ground measure of severity, the Composite Burn Index. Pages LA8–LA15 in DC Lutes, editor. FIREMON: Fire Effects Monitoring and Inventory System. USDA Forest Service, Rocky Mountain Research Station, Fort Collins, Colorado, USA.

Kuhn, M., & Johnson, K. (2013). Applied predictive modeling (Vol. 26): Springer.

Loboda, T., O'neal, K., & Csiszar, I. (2007). Regionally adaptable dNBR-based algorithm for burned area mapping from MODIS data. Remote Sensing of Environment, 109(4), 429-442.

Louppe, G., Wehenkel, L., Sutera, A., & Geurts, P. (2013). Understanding variable importances in forests of randomized trees. Paper presented at the Advances in neural information processing systems.

Meinshausen, N. (2006). Quantile regression forests. Journal of Machine Learning Research, 7(Jun), 983-999.

Meng, R., Wu, J., Schwager, K. L., Zhao, F., Dennison, P. E., Cook, B. D., . . . Serbin, S. P. (2017). Using high spatial resolution satellite imagery to map forest burn severity across spatial scales in a Pine Barrens ecosystem. Remote Sensing of Environment, 191, 95-109.

Mitrakis, N. E., Mallinis, G., Koutsias, N., & Theocharis, J. B. (2012). Burned area mapping in Mediterranean environment using medium-resolution multi-spectral data and a neuro-fuzzy classifier. International Journal of Image and Data Fusion, 3(4), 299-318.

Neyisci, T., Sirin, G., Bas, M. N., & Saribasak, H. (2016). Antalya - kumluca ve adrasan orman yanginlari hakkinda rapor.

Palandjian, D., Gitas, I. Z., & Wright, R. (2009). Burned area mapping and post-fire impact assessment in the Kassandra peninsula (Greece) using Landsat TM and Quickbird data. Geocarto International, 24(3), 193-205.

Pereira, J. M. (1999). A comparative evaluation of NOAA/AVHRR vegetation indexes for burned surface detection and mapping. IEEE Transactions on Geoscience and Remote Sensing, 37(1), 217-226.

Petropoulos, G. P., Kontoes, C., & Keramitsoglou, I. (2011). Burnt area delineation from a uni-temporal perspective based on Landsat TM imagery classification using support vector machines. International Journal of Applied Earth Observation and Geoinformation, 13(1), 70-80.

Petropoulos, G. P., Vadrevu, K. P., Xanthopoulos, G., Karantounias, G., & Scholze, M. (2010). A comparison of spectral angle mapper and artificial neural network classifiers combined with Landsat TM imagery analysis for obtaining burnt area mapping. Sensors, 10(3), 1967-1985.

Phiri, D., & Morgenroth, J. (2017). Developments in Landsat Land Cover Classification Methods: A Review. Remote Sensing, 9(9).

Pinty, B., & Verstraete, M. (1992). GEMI: a non-linear index to monitor global vegetation from satellites. Plant ecology, 101(1), 15-20.

Ramo, R., & Chuvieco, E. (2017). Developing a Random Forest Algorithm for MODIS Global Burned Area Classification. Remote Sensing, 9(11), 1193.

Schepers, L., Haest, B., Veraverbeke, S., Spanhove, T., Vanden Borre, J., & Goossens, R. (2014). Burned area detection and burn severity assessment of a heathland fire in Belgium using airborne imaging spectroscopy (APEX). Remote Sensing, 6(3), 1803-1826.

Smith, A., Drake, N., Wooster, M., Hudak, A., Holden, Z., & Gibbons, C. (2007). Production of Landsat ETM+ reference imagery of burned areas within Southern African savannahs: comparison of methods and application to MODIS. International Journal of Remote Sensing, 28(12), 2753-2775.
Stumpf, A., & Kerle, N. (2011). Object-oriented mapping of landslides using Random Forests. Remote Sensing of Environment, 115(10), 2564-2577.

Trigg, S., & Flasse, S. (2001). An evaluation of different bi-spectral spaces for discriminating burned shrub-savannah. International Journal of Remote Sensing, 22(13), 2641-2647.

Tucker, C. J. (1979). Red and photographic infrared linear combinations for monitoring vegetation. Remote Sensing of Environment, 8(2), 127-150.

Vallejo, V. R., Arianoutsou, M., & Moreira, F. (2012). Fire ecology and post-fire restoration approaches in Southern European forest types. In Post-fire management and restoration of southern European forests (pp. 93-119): Springer.

Varamesh, S., Hosseini, S. M., & Rahimzadegan, M. (2017). Comparison of Conventional and Advanced Classification Approaches by Landsat-8 Imagery. Applied Ecology and Environmental Research, 15(3), 1407-1416.

Wilson, E. H., & Sader, S. A. (2002). Detection of forest harvest type using multiple dates of Landsat TM imagery. Remote Sensing of Environment, 80(3), 385-396.

Zhang, Y. (2002). A new automatic approach for effectively fusing Landsat 7 as well as IKONOS images. Paper presented at the Geoscience and Remote Sensing Symposium, 2002. IGARSS'02. 2002 IEEE International.

International Journal of Engineering and Geosciences (IJEG),
Vol; 4, Issue; 2, pp. 088-093, June, 2019, ISSN 2548-0960, Turkey,
DOI: Your 10.26833/ijeg.473944

THE DEFORMATION ANALYSIS USING HYPOTHESIS TESTS.

Ulku Kirici Yildirim[1]* and Yasemin Sisman[1]

[1]Ondokuz Mayis University, Engineering Faculty, Department of Geomatic Engineering, Samsun, Turkey (ulku.kirici/ ysisman@omu.edu.tr); **ORCID 0000-0002-3569-4482; ORCID 0000-0002-6600-0623**

*Corresponding Author, Received: 24/10/2018, Accepted: 25/02/2019

ABSTRACT: There are temporary or permanent physical changes depending on time in earth surface. These physical changes named as deformation. The magnitude and direction of the deformation effect must be measured and controlled. The geodetic deformation network is established to determine the deformation movements and the deformation measurements are made. Then, the point coordinates are calculated used the free network adjustment. So, the different point coordinates were obtained according to measured time. The difference of point coordinate must be test to decide as significant or insignificant. Thus, the significance test based hypothesis test can be made. In this study, deformation network was established in Toybelen village of Samsun province and the deformation measurements were made periodically. The deformation network was create with using 15 points and one of these point is the control point. This deformation network measured in two periods used the global positioning system. Evaluation was made using the Topcon program and point coordinates were obtained. Differences in point coordinates received and these differences were significant tested. The program written in the matlab program was used for this test. Finally, coordinate values compared in two periods and movement points have been identified.

Keywords: *Deformation, Hypothesis Tests, Significant Tests, Outlier Measurement Tests*

1. INTRODUCTION

Deformation is defined as shape changes that occur in or around major engineering structures due to tectonic plate movements, landslides, displacement of the earth core, or artificial events caused by human hands. Measurement made at different periods for monitoring these changes are called deformation measurements. The determination and interpretation of these changes is called deformation analysis (Tanır, 2000). The aim of deformation analysis is the detection; localization and modelling of point movements in multiply measured networks. Such an analysis provides valuable information about the deformations of physical and man-made objects on the earth surface. In the deformation studies, geodetic observations are repeated at different epochs of time. The observations of each epoch are adjusted independently. From coordinate differences between the epochs, the parameters of the deformation model are estimated and conclusions on the object deformations are drawn (Kaplan at al., 2004). These conclusions examine and compared.

The aim of the study is to determine the points of deformation in the study area designated as Toybelen village. Toybelen village is located in Samsun province. Firstly, the polygon network was laid in the region for this purpose. Then three periods were measured in the region and point coordinates are calculated. The significance test was applied to the calculated coordinates and the results were commented. These application were done in matlab programming language.

2. DEFORMATION ANALYSIS

Any object, natural or man-made, undergoes changes in space and time. Deformation refers to the changes a deformable body undergoes in it is shape, dimension, and position. Since the results of deformation surveys are directly relevant to the safety of human life and engineering surveying, recently deformation analysis has become more important (Kaplan et al., 2004). The changes that occur in the shape of an object, its position and its size due to any effect are called deformation. The upper layers of the earth's crust are in constant motion both horizontally and vertically due to factors such as change of ground water level, tectonic phenomena, landslides, etc. Therefore, any large man-made structures such as bridges, high rise buildings, dams, etc., which are built on the surface of the earth are subject to deformation. This deformation needs to be monitored continuously for safety assessment purpose (Setan et al., 2001)

The traditional task of deformation analysis is the investigation of movements and displacements of an object with respect to space and time. Driven by the development of measuring and analysis techniques and the need of interdisciplinary approaches for solutions, the goal of geodetic deformation analysis is nowadays to proceed from a merely phenomenological description of the deformations of an object to the analysis of the process which caused the deformations (Heunecke et al., 2000).

There are two main purpose of deformation analysis. These are:

- Geometric condition of the deformed object (location and shape change)
- To learn about physical condition (deformation relation with effective force) (Bayrak, 2003)

Deformation are analyzed in different model according to type of the problem and method of the measurement.

These models are:

- Non-time-dependent static models
- Kinematic models that depend on time and position
- Dynamic models that depend on the time and location of the cause of motion.

There are static, kinematic and dynamic models in deformation analysis. The static deformation model consists in a purely geometrical comparison of the state of an object represented by its characteristic points at different time periods. Such kind of deformation analysis is applied by the geodetic network method in geodesy.

The stages in determining deformations by using the geodetic network method are as follows:

- Setting up monitoring networks: A monitoring network, which consists of deformation control points which are established on the object under investigation and control points which are established out of the stable area, is set up according to optimum aim functions.
- Taking observations: The periodic measurements are conducted within a determined periodic interval on monitoring network.
- Evaluating observations: In advance of deformation analysis, free network adjustment which shows realistic form internal precision of network is performed.
- Deformation analysis: Deformation analysis is made using coordinates of different periods with a suitable static deformation method and the results are interpreted (Tanır Kayıkçı et al., 2012)

Also, the deformation monitoring can be determinate with significance test of coordinate difference. The significance test is an application of hypothesis test.

2.1 Hypothesis Test

The proposed solution of scientific methods is expressed in practice in the form of hypothesis and research questions. So the hypothesis is simply an assertion a theory. As a solution, this claim is tried to be confirmed. The process of establishing a hypothesis and confirming or falsifying this hypothesis and reaching a decision at the end is called the hypothesis test. Establishing a hypothesis; expresses the determination of two propositions which are complementary to each other. So hypotheses in hypothesis tests are expressed by two propositions. The first of them is expressed by 'null hypotheses', 'H_0'. The second proposition is the expression 'H_1', which is called 'alternative hypothesis'(Demir, 2017).

A statistical test method can be briefly summarized as follows:

•Establishment of zero hypothesis H_0 and alternative hypothesis H_1

Bi-directional hypothesis testing

$$H_0 : \mu = \mu_0$$
$$H_1 : \mu \neq \mu_0$$

Unidirectional of Hypothesis Tests

$$H_0 : \mu = \mu_0 \qquad H_0 : \mu = \mu_0$$
$$H_1 : \mu > \mu_0 \ \text{ or } \ H_1 : \mu < \mu_0$$

•Generation of known distribution test value with using data

•Choice of probability of error α and production of limit values of test size using distribution rulers

•Determining whether the size of the test is in the Acceptance Zone or the Red Zone

2.1.1 Model Hypothesis Testing

Model hypothesis testing should be performed before proceeding to deformation analysis. The modeling hypothesis test is used to check whether the relations between the measurements and the unknowns are appropriate in the adjustment, the sensitivities of the measures and the correlations between them.

As a result of evaluation of similar conditions and same kind of measurements, root mean square error finding before adjustment is a priori (s_0) value, root mean square error finding after adjustment is a posteriori (m_0) value (Ünver et al., 2015).

Null hypothesis for model hypothesis testing;

$$H_0 : E\{m_0^2\} = E\{s_0^2\} = \sigma_0^2$$

Alternative hypothesis in one-way tests,

$$H_{S_1} : E\{m_0^2\} < E\{s_0^2\}$$

or

$$H_{S_1} : E\{m_0^2\} > E\{s_0^2\}$$

is established. Two-way tests,

$$H_{S_2} : E\{m_0^2\} \neq E\{s_0^2\}$$

is established as the formula.

Determined Test Value "Eq. (1)";

$$T = \frac{m_0^2}{s_0^2}; \qquad m_0 > s_0 \tag{1}$$

Then it is compared then Table value "Eq. (2)".

$$q_1 = F_{f_1, f_2, 1-\alpha} \ \text{or} \ q_2 = F_{f_1, f_2, 1-\frac{\alpha}{2}} \tag{2}$$

If the test value is smaller than the table value (T < q), the adjustment model is valid; if it is greater (T > q) the adjustment model is not valid (Bayrak, 2003).

2.1.2. Outlier measurement test

No matter how careful deformation measurements are made, errors that occur during measurements cannot be prevented. However, if these errors are not detected during the evaluation of the measurements, they cause to a wrong conviction about the presence and direction of the deformation. These errors, which lead to the invalidity of the mathematical model of the adjustment, can be eliminated by an outlier measurement tests. The aim of the outlier measurement tests is to determine a measure, which is the largest correction. After the outlier with the largest amount of error is determined and eliminated, the remaining other measures are re-tested again, and this process is continued until the outlier measurements end (Bayrak, 2003; Tanır, 2000).

The differences between the adjustment coordinates obtained after removal of the outlier measurements in each period may not yet reflect the full-scale deformation due to random errors in the measurements. In this case, to analyze the significance of the changes in the coordinates, deformation analysis is carried out in which the coordinate differences are tested by statistical methods (Altıntaş, 2014).

2.1.3. Static significance test

Static model is the most basic method whether motion occurs in the object and determining the point coordinate differences determined at various periods of the deformation network including the object and it surroundings with statistical significance test (Bayrak., 2003). To determine movements with a static model, a deformation network is measured at different observation times with geodetic methods. A functional model, solved according to the least squares method, is constituted for each observation period. Thus, coordinate vectors (x_1 and x_2), their variance– covariance matrices ($Q_{x_1x_1}$ and $Q_{x_2x_2}$) and the sum of squares of residuals to be added to observations ($v_1^T p_1 v_1$ and $v_2^T p_2 v_2$) for the t_1 and t_2 periods are computed separately.

Then, the coordinate difference vector (d) is computed as follows "Eq. (3)".

$$d = x_1 - x_2 \tag{3}$$

The covariance matrix (Q_{dd}) of vector d is calculated as follows "Eq. (4)":

$$Q_{dd} = Q_{x_1x_1} + Q_{x_2x_2} \tag{4}$$

Root mean square error "Eq. (5)";

$$m_0 = \sqrt{\frac{V_1^T V_1 + V_2^T V_2}{(n-u+d)+(n-u+d)}} \tag{5}$$

Test value for a hypothesis test "Eq. (6)";

$$T = \frac{d}{m_0\sqrt{Q_{dd}}} \tag{6}$$

International Journal of Engineering and Geosciences (IJEG),
Vol; 4, Issue; 2, pp. 088-093, June, 2019,

Table value;

$$f = f_1 + f_2 \tag{7}$$

$$f_i = n_i - u_i + d \tag{8}$$

$$h = rang(Q_{x_1x_1}) = rang(Q_{x_2x_2}) \tag{9}$$

$$q = F_{h,f,1-\alpha} \tag{10}$$

are determined.

If the test value (T) is greater than the F-distribution table value, the null hypothesis is rejected and point positions probably change (Yalçınkaya et al., 2004). But if F-distribution table value is greater than test value (T) null hypothesis is true and there is no movement in point positions.

3. APPLICATION AND RESULTS

In this study landslide area in Toybelen village of Atakum district of Samsun province was chosen as study area. Firstly, a polygon network consisting of 15 points has been laid. One of these point is selected as control point. These points Show that the Figure 1 and Figure 2.

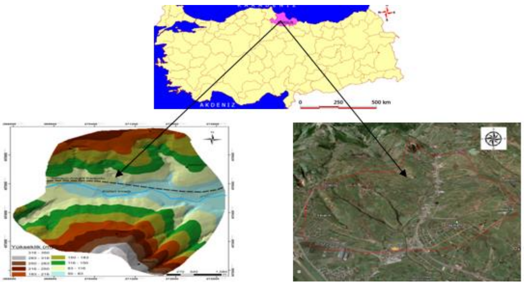

Figure.1 Application area

Figure 2: Study area

Three periods of measurements were made on the study area approximately four months apart. These measurements were made in static measurement method. After measurements were completed, post processing was done in the Topcon Tools. The data were evaluated in Matlab programming language and the results were compared. The version of the matlab program used is MatlabR2017a. The Matlab program used is licensed by Ondokuz Mayis University. Then coordinates and the varyans-covaryans matrix of the points were calculated with the measurements. d differences were calculated and significant test was made for these differences. Finally, Test value (T) and Table value (q) were obtained.

The results obtained are as in the following table. The first three columns in table show that determined test value (T) comparison first and second period measurement in application. Other measurement shows that comparison first and third period measurement in application.

Table 1 Calculated Test Value (TV)

	First and Second Period Measurements			First and Third Period Measurement		
	TV(x)	TV(y)	TV(z)	TV(x)	TV(y)	TV(z)
1	1.628	1.928	4.582	7.417	2.830	0.247
2	1.628	1.427	14.949	0.961	2.417	13.076
3	6.085	2.983	0.857	46.976	12.829	0.302
4	19.142	0.789	1.239	106.863	2.005	7.664
5	4.722	1.496	3.583	13.418	6.313	4.267
6	2.379	5.058	0.576	3.709	10.659	6.566
7	2.504	2.053	1.077	2.335	6.950	5.329
8	2.629	0.576	11.693	3.022	4.066	4.423
9	1.502	2.053	14.473	3.434	1.181	11.373
10	8.388	5.584	9.440	82.963	20.109	30.932
11	1.753	2.329	0.926	28.570	5.549	3.681
12	6.015	1.063	14.796	5.389	1.606	9.546
13	0.601	2.546	9.864	18.917	1.606	3.651
14	0.902	1.363	3.970	15.617	9.524	4.971
P001	15.109	6.431	6.043	15.726	1.105	22.866

After the test values are calculated, the table value is passed. The table value (q) found as 6.35 in the study. Then the table values and test values were compared. The points whose test value (T) is greater than table value (F) are marked. Then in both periods, the points that are greater than the test value are marked. These value are shown that Table 2.

Table 2: Points that move in both periods

	First and Second Period Measurements			First and Third Period Measurement		
	TV(x)	TV(y)	TV(z)	TV(x)	TV(y)	TV(z)
1	1.628	1.928	4.582	7.417	2.830	0.247
2	1.628	1.427	14.949	0.961	2.417	13.076
3	6.085	2.983	0.857	46.976	12.829	0.302
4	19.142	0.789	1.239	106.863	2.005	7.664
5	4.722	1.496	3.583	13.418	6.313	4.267
6	2.379	5.058	0.576	3.709	10.659	6.566
7	2.504	2.053	1.077	2.335	6.950	5.329
8	2.629	0.576	11.693	3.022	4.066	4.423
9	1.502	2.053	14.473	3.434	1.181	11.373
10	8.388	5.584	9.440	82.963	20.109	30.932
11	1.753	2.329	0.926	28.570	5.549	3.681
12	6.015	1.063	14.796	5.389	1.606	9.546
13	0.601	2.546	9.864	18.917	1.606	3.651
14	0.902	1.363	3.970	15.617	9.524	4.971
P001	15.109	6.431	6.043	15.726	1.105	22.866

Thus in three periods of measurements;

- z axis of point 2
- x axis of point 4
- z axis of point 9
- x and z axis of point 10
- z axis of point 12
- x axis of point P001

motion detected.

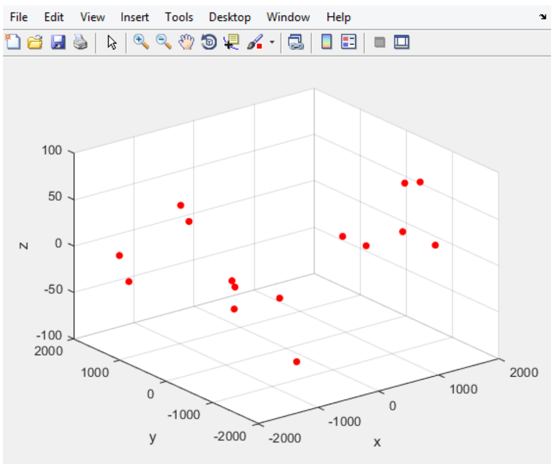

Figure 3. Plotted point distributions in Matlab

4. DISCUSSION AND EVALUATION

When looking at the values, there was no motion detection in y axis. Generally, it seen that movement in the z axis. Also the application period progresses were observed that the test values of the detected points were increased. When the movement observed point is looked, it is observed that the values in point x and y axis in point 2 are very small but move in z axis. Point 4 has only movement in the x axis but test value was seen to increase too much in these axis. Points 1, 5, 6, 7 and 8 are close to each other when looking at the study area. No motion was observed at these points. Point 9 has only movement in the z axis. Point 10 has been observed motion in both x and z axis. At point 10, the test values were seen to increased too much in x and z axis. Point 12 has only movement in the z axis and lastly point P001 has only movement in the x axis. It is seen that the test values of point P is very close to each other in two evaluations.

In this study, three period measurement were done and finding these results. The results obtained are initial results. It is necessary to increase the number of measurements and continue to work. As the number of measurement periods increases, the continuity of the observed points will occur. Thus, if there is a danger in the region, it will be revealed and necessary precautions can be taken.

REFERENCES

Altıntaş F. (2014). Gümüşhane –Trabzon Hattı Boyunca Yerkabuğu Hareketlerinin GNSS Verileri İle İzlenmesi, Yüksek Lisans Tezi, Fen Bilimleri Enstitüsü, Gümüşhane Üniversitesi, Gümüşhane.

Bayrak T. (2003). Heyelanlar için Bir Dinamik Deformasyon ve Bir Dinamik Hareket Yüzeyi Modelinin Oluşturulması, Doktora Tezi, Fen Bilimleri Enstitüsü, Karadeniz Teknik Üniversitesi, Trabzon.

Demir E. (2017). İstatistik Ders Notları [PDF belgesi]. Online Web site: 12 Temmuz 2018 tarihinde http://www.academia.edu/30931820/Istatistik_Ders_Notlarim_E.Demir_2017_.pdf adresinden erişildi.

Heunecke O., Welsch W. (2000). Terminology and Classification of Deformation Models in Engineering Surveys, Journal of Geospatial Engineering, Vol. 2, No.1, pp.35-44, Hong Kong.

Kaplan M.O., Ayan T., Erol S. (2004). The Effects of Geodetic Configuration of the Network in Deformation Analysis, FIG Working Week 2004 Athens, Greece, May 22-27, 2004.

Setan H.,Singh R. (2001). Deformation Analysis Of A Geodetic Monitoring Network, Geomatica. Vol. 55, No. 3.

Tanır E. (2000). Deformasyon Analizinde Statik Değerlendirme Yöntemleri, Yüksek Lisans Tezi, Fen Bilimleri Enstitüsü, Karadeniz Teknik Üniversitesi, Trabzon.

Tanır Kayıkçı E., Yalçınkaya M. (2012). Determination of Horizontal Movements by Static Deformation Models: A Case Study on the Mining Area, Experimental Techniques 39 (2015) 70–81.

Ünver Ö.,Gamgam H.,Altunkaynak B. (2015). Temel İstatistik Yöntemler, Seçkin Yayınevi.

Yalçınkaya M., Bayrak T. (2004). Comparison of Static and Dynamic Geodetic Deformation Models for Kutlugün Landsline in Northeastern Turkey, Natural Hazards (2005) 34: 91–110.